ISSN 0429-8284

Whole Number 206

e-Front runners

FUJI ELECTRIC REVIEW

3

2004 VOL.50

Latest Research and Development

Fuji Electric Group

e-Front runners

Environment, information, services and components are the keywords for which Fuji Electric is applying its creative technical development capability.

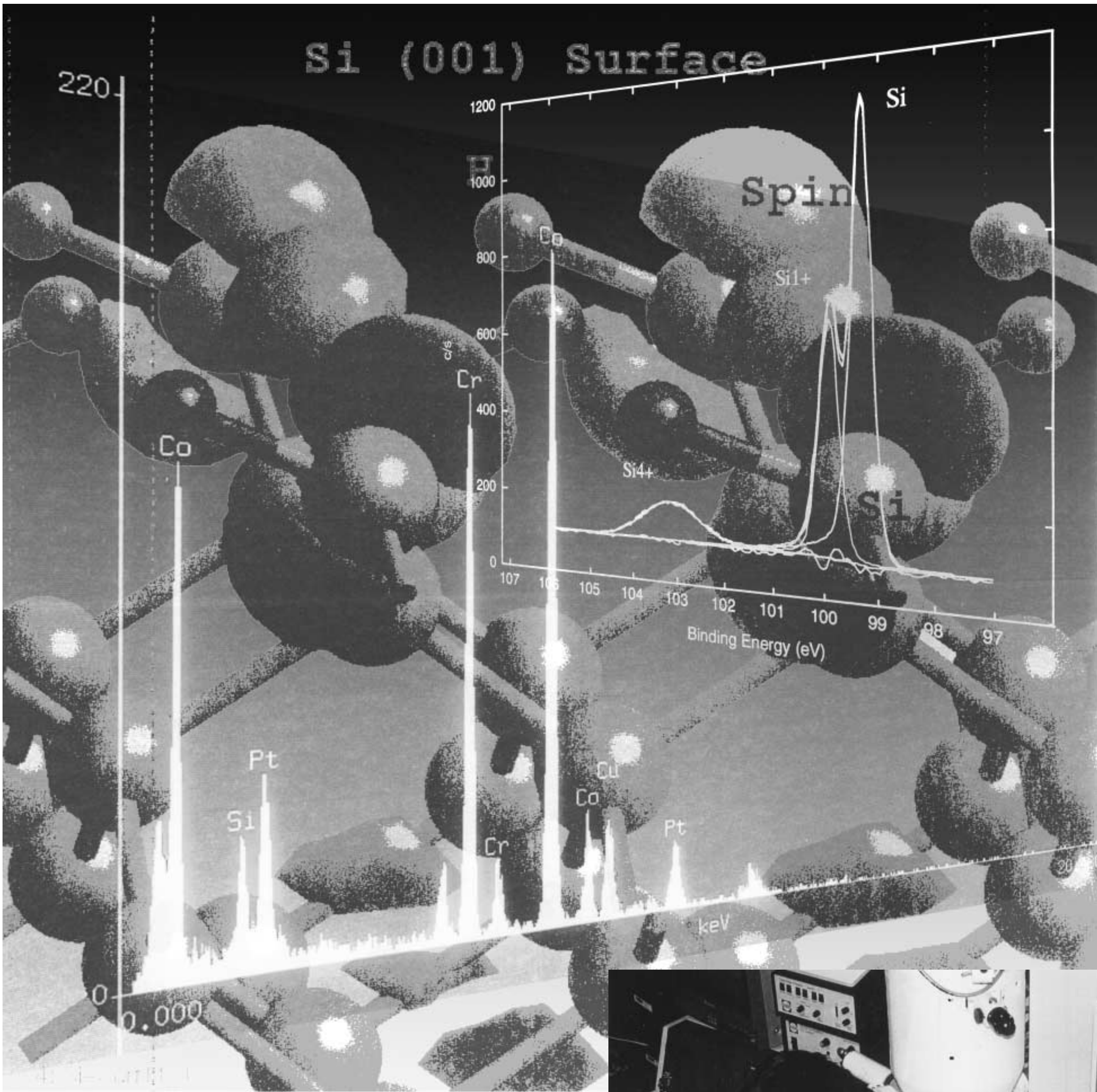

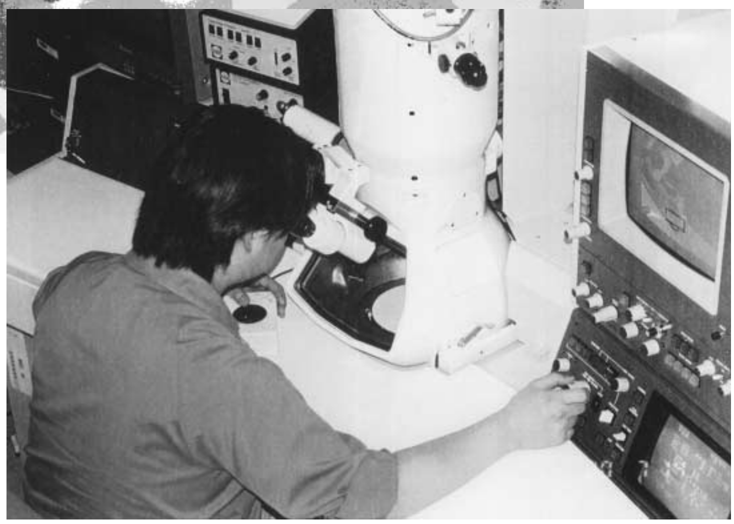

In order to help to build a vibrant and prosperous society, Fuji Electric intends to continue providing technology and constructing systems in harmony with the global environment.
To advance the realization of this purpose, Fuji Electric is applying its basic research capability to the control of molecules and atoms. This basic research will lead to the discovery and understanding of physical properties and phenomena of new materials and will open the door to an era of new technology.

Fuji Electric Advanced Technology Co., Ltd.

FUJI ELECTRIC
REVIEW

3

2004 VOL.50

Latest Research and Development

CONTENTS

Cover photo:

With the spread of globalization, competition among companies is becoming increasingly intense. Under the current circumstances, manufacturers are categorized as either winners or losers based on their business performance, and only those companies possessing genuine technical strength will survive. R&D truly represents a lifeline for manufacturers.

In addition to developing products directly related to its business, Fuji Electric is also advancing the basic research and technical development for next generation products and new businesses. Fuji aims to establish novel proprietary technology and is also concentrating its efforts on analysis, evaluation and simulation techniques in order to improve the efficiency of development processes.

Symbolizing the creation of new products from basic research, the cover photo shows images of the color-conversion organic EL device and lateral trench MOSFET that are presently under development and an optimization technique based on meta-heuristics, all of which are superimposed against a background of thin film deposition equipment.

Fuji Electric Holdings Co., Ltd. Head Office : No.11-2, Osaki 1-chome, Shinagawa-ku, Tokyo 141-0032, Japan

Electrical Bistable Devices Using Organic Materials

Haruo Kawakami
Hisato Kato
Keisuke Yamashiro

1. Introduction

In development of new products in the field of electronics technology, new materials with high performance are strongly required. Although organic electrical materials have not yet reached the basic performance level of silicon, they are promising to various applications because of their advantages such as good light interaction, low cost processing, suitability for large area devices, and the like. Figure 1 lists product groups in the burgeoning field of information devices together with new device technologies for which application is expected. Organic electrical materials account for a large percentage of these new technologies.

Fuji Electric holds a large share of the global market for organic photoconductors and is presently developing organic light emitting diodes (OLEDs) as next generation products. Organic electrical material forms the basis for these business areas, and advancement of its development is important.

This paper describes the present status and future trends of bistable devices, which are being developed as next generation devices that utilize organic electrical materials.

Fig.1 Technical trends of information device and new technology

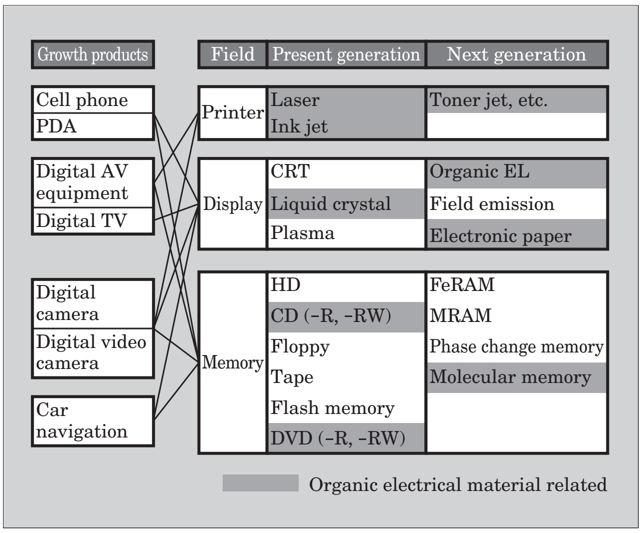

2. Features of Organic Electrical Materials

Table 1 compares the charge mobilities of typical organic electrical materials to that of silicon. The highest mobility value is for pentacene single crystal which has a hole mobility of approximately 3.2 $cm^2/V \cdot s$. Electron mobility is even lower. For this reason, devices that use these organic electrical materials generally have a limited response performance. Moreover, some materials may become unstable when exposed to the atmosphere and must be encapsulated or stabilized in some other way. Organic electrical materials, however, have the following features that are not exhibited in conventional electrical materials and device development is being promoted to leverage these features.

(1) Materials can be designed so as to control the energy gap and the interaction with light is easily customizable.
(2) Large area devices are easy to manufacture.
(3) Low cost (spin/dip coating, etc.) processes may be utilized.
(4) New devices can be realized using the particular physical properties of organic molecules (molecular alignment, dipole moment, phase transition, etc.).

For example, the switching speed of organic bistable material described in this paper is said to be approximately 10 ns and would be sufficient for many applications.

Table 1 Charge mobility of representative organic electrical materials

Item	Silicon	Pentacene single crystal	Thiophene aligned film	Conjugated conductive polymer	Liquid crystal	Conjugated small molecule
Hole mobility ($cm^2/V \cdot s$)	450	3.2	0.1	0.1	1×10^{-3}	1×10^{-5}
Electron mobility ($cm^2/V \cdot s$)	1,500	0.5	0.02	–	1×10^{-3}	1×10^{-6}

3. Organic Bistable Materials and Development Trends

In organic electrical materials having certain chemical structure, bistability is observed in which two stable resistance values exist for a single applied voltage value. Figure 2 shows an example of those characteristics. For example, when increasing the voltage gradually from 0 V, there is almost no current flow in the low voltage region and the material remains in a high-resistance state (off-state), however, at a certain threshold voltage (V_{th2}), there is a sudden increase in current by several orders. This low-resistance state (on-state) continues even when the voltage drops below V_{th2}, but when the voltage becomes lower than another threshold voltage (V_{th1}), the material returns to the off-state.

Organic materials called "charge transfer complexes" are known as organic bistable materials that exhibit these types of characteristics. These charge transfer complexes are molecular compounds formed from the two molecules of an electron donor molecule and an electron acceptor molecule, and precise control of the composition ratio of these molecules is necessary. On the other hand, a group at the University of California has recently succeeded in achieving bistable performance, similar to that of the abovementioned charge transfer complex, with a single-component organic bistable material formed by providing an extremely thin metallic middle layer within a thin film layer of organic bistable material. With this structure, controllability of the composition is better than with the conventional two-component material of a charge transfer complex, however, the addition of the new process of fabricating a metallic middle layer adds difficulty.

Fig.2 Electrical characteristics of bistable devices

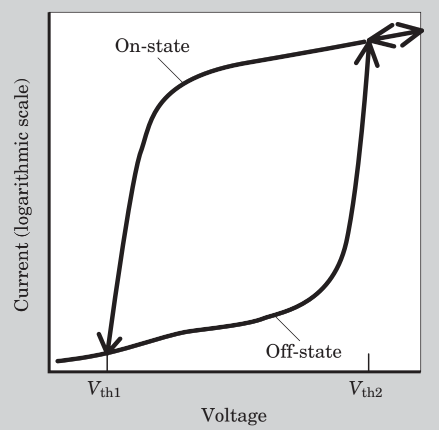

Through its development of proprietary organic bistable materials and processes, Fuji Electric has succeeded in achieving bistable performance, similar to that of the abovementioned charge transfer complex, in a single-component organic material without the provision of the abovementioned thin metal middle layer within the organic layer. This has enabled bistable devices to be made with a simple structure in which a single organic layer is sandwiched between metal electrodes.

The detailed mechanism of the bistable phenomenon in these materials is not yet well understood. In particular, there are many unknowns concerning the relatively recently developed materials that exhibit bistability in a single molecule. In the bistable devices developed by Fuji Electric, mechanisms are presumed to function such that (1) current flow is restricted by means of a charge injection barrier existing at the interface between the organic bistable material layer and the metal electrode (off-state), (2) charge accumulates at the charge injection barrier and causes the electric field to increase locally, and (3) the rise in electric field causes the charge injection barrier to

Table 2 Representative bistable devices

Organization	Material	Summary	Current density (mA/cm^2)	Switching voltage (V)	On/off ratio	Reference
Indian A.C.S	Rose, Bengal, etc./dye	Electrostatic self-assembled film, spin coated film	0.3	4.5	10^5	(6)
Univ. of Wales	Thiophene polymer	ITO/electrochemical deposition/Al	0.004	5.0	10	(7)
Kyushu Univ.	Melamine cyanurate	Evaporated film	16.0	12.0	10	(8)
Chitose Institute of Science	Cu–TCNQ	Evaporated film	8.0	10.0	10^2	(9)
Univ. of California	AIDCN	Evaporated film	100.0	3.0	10^6	(4)
Yale Univ., Rice Univ.	Nitro-amino molecule	Self-assembled monolayer	–	5.0	–	(12)
Hewlett Packard	rotaxanes	Self-assembled monolayer	–	1.5	10^3	(13)
Fuji Electric	DODMT	Evaporated film	2.0	20.0	10^3	(6)
Philips	ZnCdS	Sputtered film	80.0	0.5	10^6	(10)
Tokyo Univ. of Agriculture and Technology	porous Si	–	1.0	17.0	10^5	(11)

collapse and charge to flow toward the organic bistable material film (transition from off-state to on-state). However, there are many remaining issues to be investigated concerning details of the characteristics and their relation to the physical properties of the organic materials.

This bistability is suitable for application to high density recording media and switching devices and, in recent years, there has been an increase in the number of organizations pursuing development of this technology. In addition to organic materials, inorganic materials should also be developed and materials development is ongoing. Major developments of bistable devices are listed in Table 2.

4. Development and Results at Fuji Electric

Fuji Electric is promoting the development of devices that utilize this bistability. Since these device use organic material as a raw material, the manufacture of large area devices at low-temperature processes is possible. Moreover, since theses devices may also be used with a plastic substrate, they are believed to be particularly well suited for application to the driving devices for organic EL or other types of display panels.

At present, display panel driving methods are classified as either a passive matrix method that causes each pixel to emit light in a time-sequential manner or an active matrix method in which a control circuit is provided at each pixel to continuously emit light. In the passive matrix method, since pixels in the panel are illuminated sequentially in rows, the duration of light emission is limited for the light-emitting element of each pixel and it is necessary to instantaneously emit a bright light for the duration of the light emission. Accordingly, lower cost is possible, but there are problems involving power consumption and lifespan. On the other hand, in the active matrix method, each pixel is provided with a control circuit formed from a thin film transistor or the like, and since the light emitting state can be maintained continuously, it is acceptable for the light-emitting element of each pixel to have a low average brightness when lighted. In general, as the brightness level of organic EL material decreases, both the emitting efficiency and the light emission lifespan increase and although this is advantageous in terms of power consumption and lifespan, the high cost is a disadvantage.

However, by connecting an organic EL device in series with a bistable device as shown in Fig. 3 for example, and applying a bias voltage at both ends to maintain the on/off-state of the bistable device, light emission can be made continuous even with a structure similar to that of the passive matrix method. The on/off-state is switched by applying control pulse voltages that correspond to each switching voltage. As a result, the power consumption and lifespan of the display can be improved without the use of an expensive control circuit.

Fig.3 Configuration in which a bistable device is connected in series to an organic light emitting diode

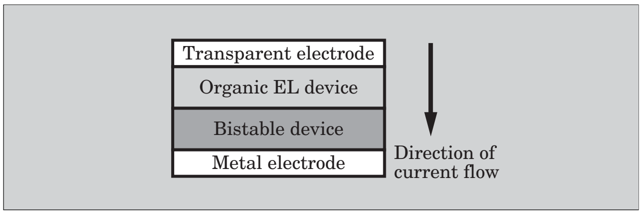

Fig.4 Operating condition of the bistable device and organic light emitting diode

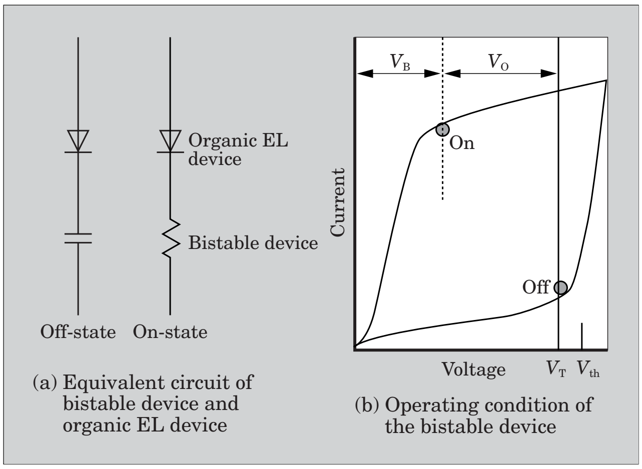

Figure 4 shows details of the operation of a pixel in which the abovementioned organic EL device is connected in series with a bistable device. When the bistable device is in the on-state, the voltage V_T applied to both devices is divided according to the resistive values of the bistable device and organic EL device. If the respective voltage values at this time are V_B and V_O, then V_O becomes the operating voltage of the organic EL device and generally requires a voltage of approximately 10 V (max.). In the off-state, the bistable device is equivalent to a capacitor and the entire V_T across both devices is applied to the bistable device. For the bistable device to be in a stable state, the voltages V_B (on-state) and V_T (off-state) applied to both states must be within the range of the abovementioned V_{th1} and V_{th2}. In other words, in order to support the driving voltage and current of the organic EL device in this application, the switching voltage V_{th2} from the off-state to the on-state must be greater than V_T (typically 15 V or higher) and the on-state must have a high current density. Using originally developed organic bistable materials, Fuji Electric has realized bistability with a single-component, single-layer structure and with this type of device, has achieved the world's highest switching voltage V_{th2} of 20 V.

Figures 5 and 6 show example characteristics of these bistable devices. Figure 5 shows characteristics

Fig.5 Electrical characteristics of bistable devices (single-layer structure)

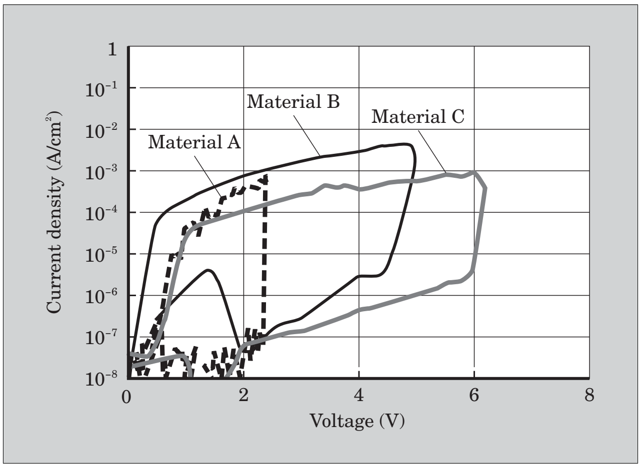

Fig.6 Electrical characteristics of bistable devices (material C)

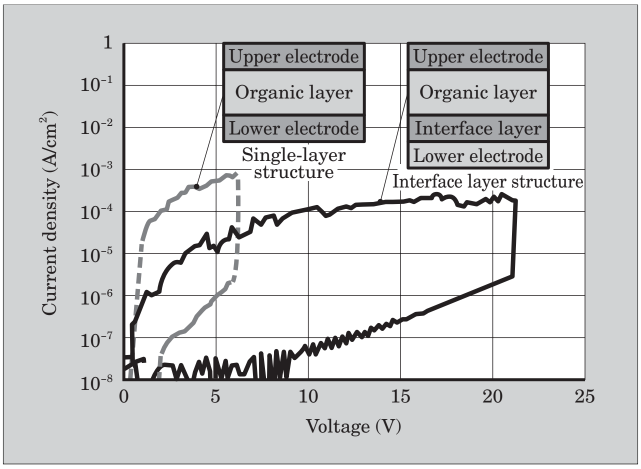

of various materials in a single-layer structure. Fuji Electric was able to achieve bistability with material A, which had previously achieved bistability only with a middle layer structure, in a simple single-layer structure (in which the organic bistable material layer is sandwiched by metal electrodes). Materials B and C are organic bistable materials that Fuji Electric has developed originally. Material B conducts positive charges (holes) and will provide a higher current than material A. Material C conducts negative charges (electrons). In the case where an organic EL device is to be connected, these materials having different polarities may be selected for use according to the device configuration. Figure 6 shows characteristics of a device that uses material C and is provided with an interface layer between the electrode and the organic bistable material layer. The switching voltage from an off-state to an on-state has been successfully improved to 20 V or higher with this configuration. The interface layer is organic material in which conductive nano-particles have been dispersed and which functions to bear a portion of the voltage applied to the bistable device and also to boost the switching voltage

Fig.7 Overview of performance of bistable characteristics

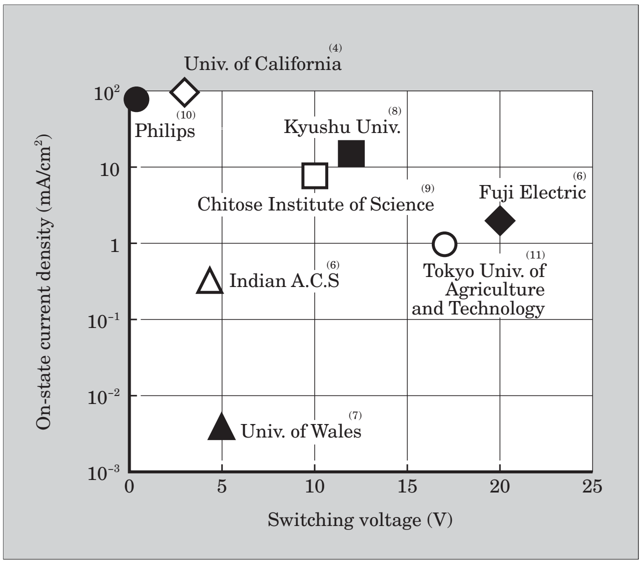

by controlling the injection of charge to the device.

Figure 7 compares the switching voltages and on-state current densities of bistable devices that have been publicly reported by various research organizations. The highest switching voltage was achieved with material C using Fuji Electric's interface structure and the highest on-current density was achieved with material A using the University of California's middle layer structure. Fuji Electric is aiming to improve the characteristics even further and is continuing its efforts to develop new organic materials and to optimize layer configurations.

5. Conclusion

This development work has only just begun and many unresolved issues remain. In particular, during the on-state, in addition to current density, issues relating to reliability and stability, such as repetition durability, environmental dependence and so forth, are expected to be difficult to resolve. Moreover, an understanding of the mechanism behind the phenomenon of bistability is crucial for resolving these technical issues, but as mentioned above, there are many unknowns surrounding this issue at present. In order to resolve these issues, in addition to in-house efforts, broad ranging cooperation with various external organizations will be indispensable. In the future, while seeking this cooperation, we intend to advance development towards the goal of practical applications.

Reference

(1) Potember, R.S. et al. Electrical switching and memory phenomena in Cu-TCNQ thin films. Appl. Phys. Lett.vol.34, 1979, p.405-407.

(2) Kumai, R. et al. Current-induced insulator-metal transition and pattern formation in an organic charge-transfer complex. Science. vol.284, 1999, p.1645-1647.

(3) Gao, H. J. et al. Using a new kind of organic complex system of electrical bistability for ultrahigh density data storage. J. Vac. Sci. Technol. vol.B15, 1997, p.1581-1583.
(4) Ma, L. et al. Nonvolatile electrical bistability of organic/metal-nanocluster/organic system. Appl. Phys. Lett. vol.82, 2003, p.1419-1421.
(5) Kawakami, H. et al. Electrical Bistable Behavior of Organic Materials in Single Layer Structure. Proc. The International Symposium on Optical Science and Technology SPIE's 48th Annual Meeting. vol.5217, 2003, p.71-79.
(6) Bandyopadhyay, A. et al. Large conductance switching and memory effects in organic molecules for data-storage applications. Appl. Phys. Lett. vol.82, 2003, p.1215.
(7) Taylor, D. M. et al. Memory effect in the current-voltage characteristic of a low-band gap conjugated polymer. J. Appl. Phys. vol.90, 2001, p.306.
(8) Gao, X. et al. Switchable organic electroluminescence. Appl. Phys. Lett. vol.81, 2001, p.4508.
(9) Oyamada, T. et al. Switching effect in Cu:TCNQ charge transfer-complex thin films by vacuum codeposition. Appl. Phys. Lett. vol.83, 2003, p.1252.
(10) van der Sluis, P. et al. Non-volatile memory cells based on Zn_xCd_{l-x}.S ferroelectric Schottky diodes. Appl. Phys. Lett.vol.82, 2003, p.4089.
(11) Ueno, K. et al. Light-emissive nonvolatile memory effects in porous silicon diodes. Appl. Phys. Lett. vol.74, 1999, p.93.
(12) Reed, M. A. et al. Molecular random access memory cell. Appl. Phys. Lett. vol.78, 2001, p.3735.
(13) Chen, Y. et al. Nanoscale molecular-switch devices fabricated by imprint lithography. Appl Phys. Lett. vol.82, 2003, p.1610.

A New Semiconductor Device with Trench Technology

Yoshihiko Nagayasu
Kunio Mochizuki
Naoto Fujishima

1. Introduction

Fuji Electric has advanced the development of semiconductor processes by promoting the research and development of "genuinely controlled processes that do not generate defects" and "devices having decisive advantages over the competition." Using specialized equipment and concentrating on processes that involve chemical reactions such as oxide layer, etching and thin film deposition and are susceptible to problems, and by making full use of microscopic analysis techniques and pursuing the true causes of problems, Fuji Electric has realized semiconductor processes having high reliability and low defect rates.

By maximizing the usage of silicon (Si) in three-dimensions in order to bypass characteristics limits of planar on-resistance, breakdown voltage and the like, and by positioning trench technology as a core technology, Fuji has promoted the research and development of the usual trench MOSFET and also new semiconductor devices such as the trench lateral power MOS (TLPM), super junction (SJ) device, and a 700 V-class trench offset drain-lateral DMOS (TOD-LDMOS).

TOD-LDMOS is a new semiconductor device and is the first application of trench processing and the concept of using a silicon substrate in three-dimensions in order to realize high breakdown voltage. This paper describes the key supporting process technologies of trench etching technology, CVD (embedding, flattening) technology and gate oxide layer (deposition, high breakdown voltage) technology that have been developed by Fuji Electric.

2. Structure of the New Semiconductor Device (TOD-LDMOS)

In the past, a structure (offset drain area) capable of realizing a breakdown voltage of 700 V or higher required an area of approximately 60 μm length on the substrate surface as shown in Fig. 1. This is because elongation of the depletion layer (X μm) in an n-type area of low concentration can achieve a high breakdown voltage $V = \int E\ (X)\ dx$ (where E is constant, and V is large when X is large) without the maximum electric field (E_{max} V/μm) generated in the vicinity of the junction exceeding the electric field (E_c V/μm) at which a reverse current begins to flow through the Si substrate. V has the theoretical limit of $V < E_c \cdot X$, and X cannot be made shorter because this distance is absolutely essential in principle for achieving the breakdown voltage.

As shown in Fig. 2, with this new technology, a trench of depth 20 μm and width of 20 μm is formed in the silicon substrate and a U-shaped offset drain is provided along the trench to fully utilize the substrate in three-dimensions, ensure the necessary distance, and increase the level of device integration while maintaining a high breakdown voltage.

Figure 3 shows the potential distribution of the TOD-LDMOS device (spacing of the equipotential lines indicates the strength of the electric field). With an offset drain that runs alongside the trench, this structure realizes an electric field within the Si substrate that is rather uniformly relaxed, and because the maximum electric field exists in the oxide

Fig.1 Schematic cross-section of a conventional 700 V-class high voltage lateral MOS

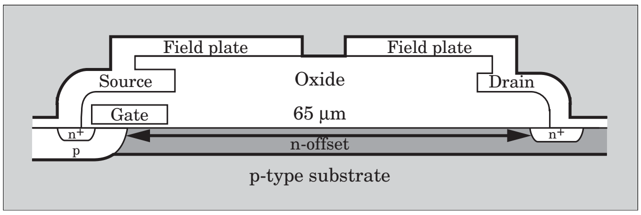

Fig.2 Schematic cross-section of the 700 V-class high voltage lateral MOS with trench technology

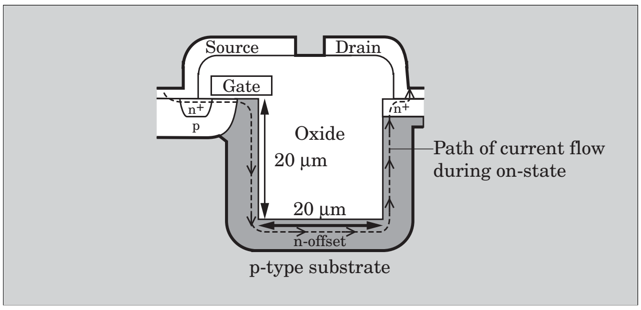

Fig.3 Simulated potential contours of TOD-LDMOS (bias voltage = 600 V, 20 V per contour)

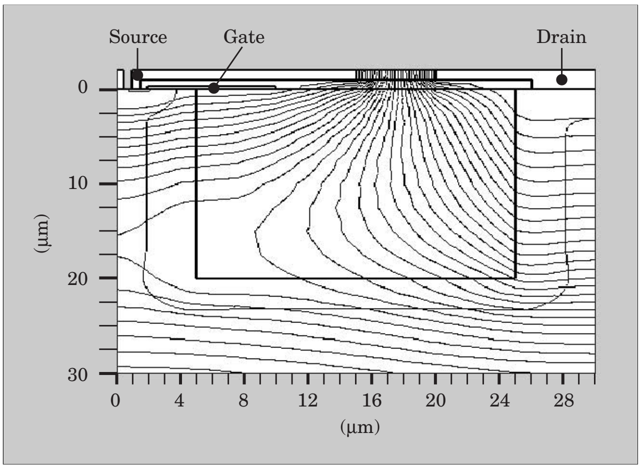

Fig.4 The silicon trench etching pattern (depth = 20 μm)

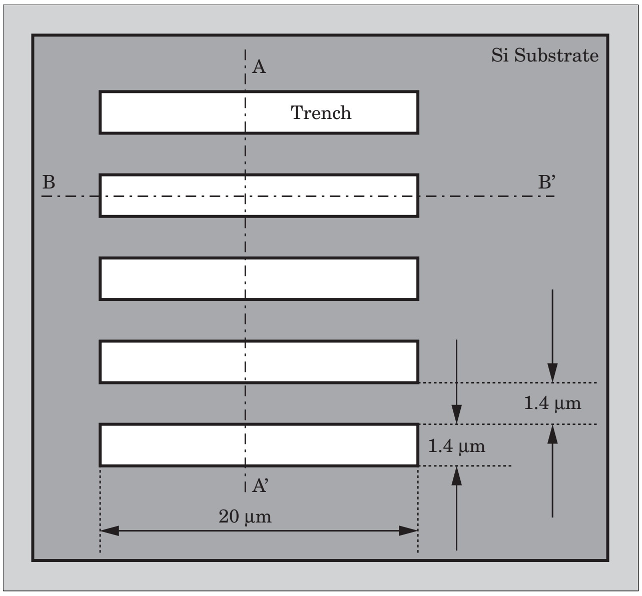

Fig.5 A schematic cross-section of a trench etching

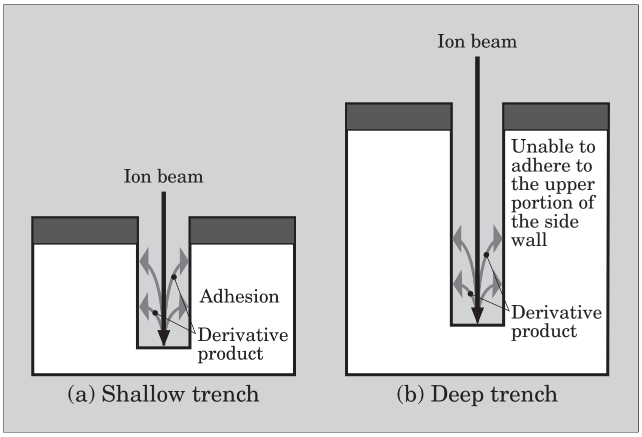

layer which has a higher breakdown voltage than Si by a magnitude of 10, breakdown does not occur even if the linear distance is short.

With this structure, however, it is necessary to form a trench that is deep and wide (20 μm × 20 μm) in the Si substrate, and then within that trench, to form a high-quality insulating region that does not cause a decrease in breakdown voltage. It is also necessary to form an offset drain region by diffusing the trench wall with a low concentration of ions. Such processing is difficult to realize, however. The desired device structure was realized by using a proprietary manufacturing method in which stripe-shaped trenches having a high aspect ratio are fabricated, oblique ion implantation is performed, and then oxidation and CVD processing are implemented to fabricate an insulating film.

3. Key Process Technologies for TOD-LDMOS

The key technologies of trench processing are described below.

(1) Formation of stripe-shaped trenches having a high aspect ratio

Figure 4 shows the shape of the trenches. Instead of forming a 20 μm × 20 μm oxide region all at once, several stripe-shaped trenches of width 1.4 μm and depth 20 μm are formed in the source-drain direction to form a sub-divided region at the realizable film thickness. We developed the following essential trench etching techniques to obtain this shape.

○ Side wall angle ≈ 90°
○ Absence of Si column residue
○ Trench side wall protection

Trench etching, as shown in Fig. 5, is performed while protecting the side wall with the derivative product (SiO_2) formed in the reaction between oxygen (O_2) contained in the etching gas and the Si substrate. At a depth of 20 μm, however, the derivative product generated at the bottom surface will be unable to adhere to the upper portion of the trench, and etching will be performed not only on the bottom surface, but also on the upper side walls. Moreover, as the etching depth increases, derivative product generated at bottom surface is not removed, and Si column residue is likely to exist. Therefore, in order to protect the sidewalls, the bias voltage applied to the Si substrate is boosted to increase the rectilinear propagation of the ion beam and reduce the portion of the beam incident on the sidewalls. Additionally, to suppress the generation of derivative products, the fluorine content of the gas is optimized to decompose solid SiO_2 into gaseous SiF_4 and O_2 to make exhausting easier. As a result, a suitable shape for this device can be obtained.

(2) Offset drain fabrication using oblique ion implantation

As shown in Fig. 6, oblique ion implantation and then thermal diffusion are performed along the trench to create an offset drain region in the trench sidewall.

Using the fact that the trench opening is long in the sideways direction, impurities are introduced by

Fig.6 Schematic cross-section of the oblique and vertical ion implantation, followed by offset drain thermal diffusion

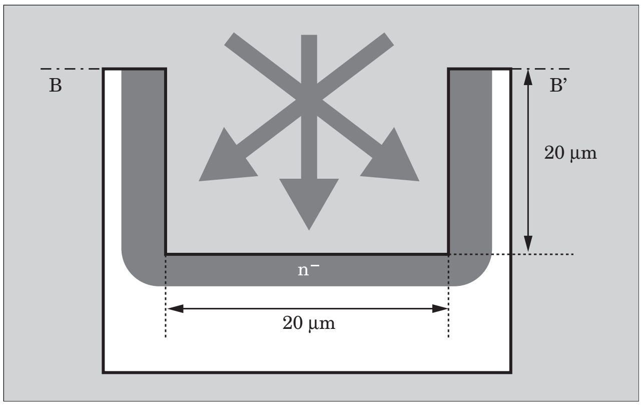

Fig.7 Oxidation of thin crenellated silicon

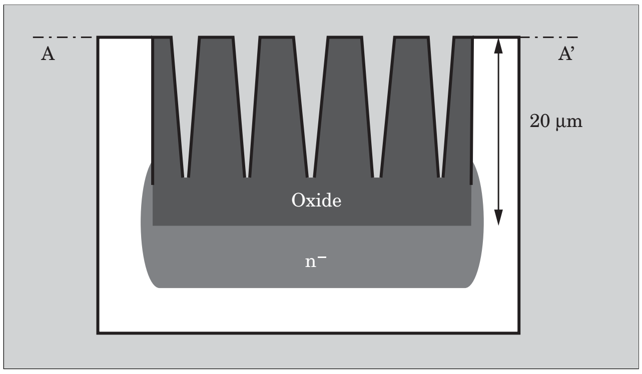

Fig.8 Deposition of oxide in the trench region

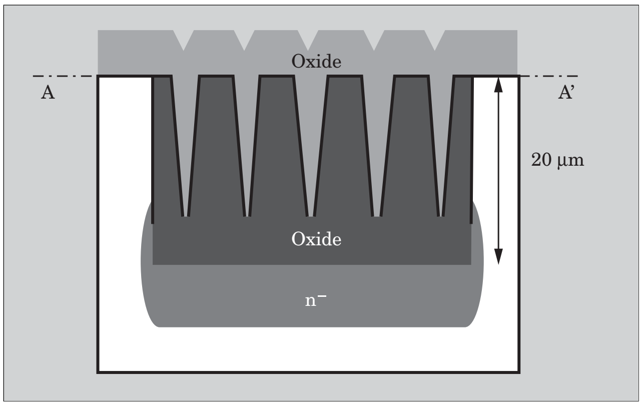

Fig.9 SEM micrograph of the fabricated TOD-LDMOS

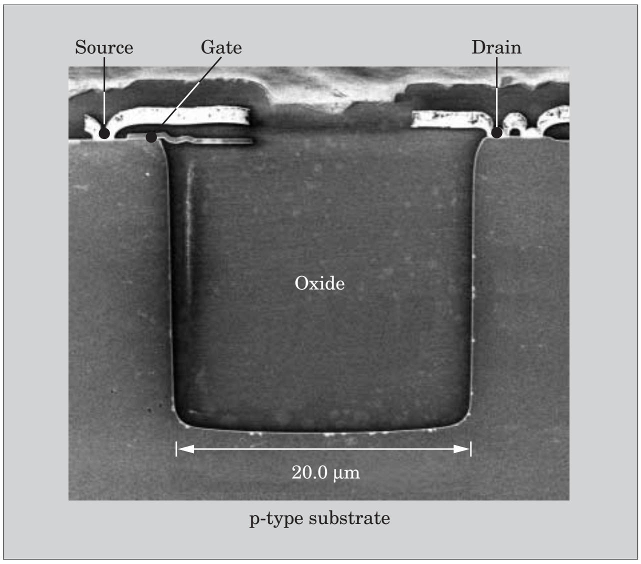

Fig.10 Relationship between specific on-resistance and breakdown voltage

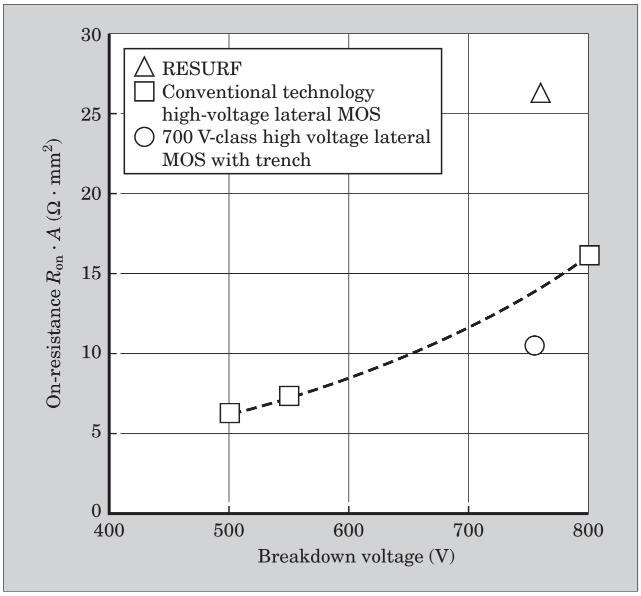

implanting ions in a direction horizontal to line segment BB’ such that ions will be implanted in the bottom surface and both sidewalls at a 45° oblique angle with relatively low fluctuation.

(3) Thermal oxidation of Si substrate material remaining between crenellated trenches

Figure 7 shows a cross-section of the thin crenellated Si substrate after thermal oxidation.

All Si material between the crenellated trenches has become oxide film (SiO_2), and the volume of SiO_2 is approximately twice that of Si. At this point in time, gaps will exist at the top of the crenellated substrate. Techniques for scientifically and accurately controlling the width of the residue of this thermally oxidized pitch and for relieving stress enable the crenellated shape to be formed without remnants of the Si core and without deformation and collapsing of the oxide film columns by the stress.

(4) Deposition of insulating film in the trench region

Figure 8 shows a cross-section of the Si substrate after deposition of an insulating film.

When insulating film (SiO_2) is deposited so as to fill up the gaps, it is important to control empty regions occurring within the deposited SiO_2 as stress-relief regions and to deposit the insulating film below the Si surface (line segment AA’). Figure 9 shows a cross-sectional photograph of an actually fabricated TOD-LDMOS device.

As a result, the output on-resistance is reduced by approximately 30 % compared to prior devices to realize 11 $\Omega \cdot mm^2$, which is the best in the industry for a device having a 750 V breakdown voltage (Fig. 10). Shrinking the device pitch enables the chip size to be reduced and the production cost of single-chip power ICs to be decreased. It is believed that these techniques will enable cost reductions in such electronic equipment as AC adapters.

4. Conclusion

In order to continue developing new devices that utilize Si in three-dimensions to the maximum extent possible, we intend fully to utilize epitaxial growth, embedding and interconnect technologies, as well as trench technology. Moreover, utilizing quantitative process design aided by the analysis of elementary process steps, visualization techniques and in-line evaluation of the etching process, enhanced washing and surface treatment technology, particle component analysis, clean room monitoring technology, and the like, we intend to revolutionize manufacturing processes, enhance the process technology of the Fuji Electric Group and contribute to the development of new products.

References

(1) Fujishima, N. et al. A Low On-resistance Trench Lateral Power MOSFET in a 0.6 µm Smart Power Technology for 20-30 V Applications. IEDM Technical Digest 2002. p.455-458.

(2) Teranishi, H. et al. A High Density, Low On-resistance 700 V Class Trench Offset Drain LDMOSFET (TODLDMOS). IEDM Technical Digest 2003. p.757-760.

(3) Wakimoto, S. et al. Characteristics of Si Trench Etching. 25th International Symposium on Dry Process (DPS 2003).

(4) Kuribayashi, H. et al. Investigation of shape transformation of silicon trenches during hydrogen annealing. To be published in Japanese Journal of Applied Physics. 2004.

(5) Ogino, M. et al. Degradation of Gate Oxide Reliability Due to Plasma-Deposited Silicon Nitride. To be published in Japanese Journal of Applied Physics. vol.43, no.3, 2004.

Structural Control Method for Perpendicular Magnetic Recording Film

Shunji Takenoiri
Yasushi Sakai
Sadayuki Watanabe

1. Introduction

The recording density for HDDs (hard disk drives) has rapidly increased at a rate of 60 to 100 % per year since 1997. The rate of increase is slowing down nowadays, but is still expected to continue at about 30 to 60 % per year in the future. As a result of this significant advancement, the method of longitudinal recording is approaching its application limits due to the phenomenon of “thermal fluctuation” in which recorded bits become unable to retain their stability. With the longitudinal recording method, as higher recording density increases, thermal fluctuation becomes larger. As a consequence, the perpendicular recording method, which has opposite characteristics to those of the longitudinal recording method, i.e. its recorded bits become more stable at higher recording densities, has been developed actively.

There have been many studies of the perpendicular recording method since it was first proposed by Iwasaki et al. in 1975(1). Even though the perpendicular recording method had obvious advantages in principle, only recently has a perpendicular medium demonstrating higher performance than a longitudinal medium been obtained. The application of CoPtCrO(2) or CoPtCr-SiO_2 to a recording layer provided the necessary breakthrough. These types of media realize enhanced grain segregation due to oxide materials that easily precipitate at the grain boundary. We have previously reported that good read-write performance and high thermal stability resulting from relatively large uniaxial anisotropy constants and a well-isolated microstructure can be obtained by using CoPtCr-SiO_2 as the recording layer instead of a conventional CoCr-based alloy, alluding to the great potential for high-density recording in the future(3). Figure 1 shows a schematic diagram of Fuji Electric perpendicular recording medium in which CoPtCr-SiO_2 and Ru are typically utilized as a recording layer and an intermediate layer, respectively.

Generally speaking, magnetically separated, uniform and fine grains for a recording layer must be made in order to obtain an excellent performance medium. To realize the above conditions, in addition to controlling the material and deposition conditions of the recording layer, the structural control of intermediate layers is also known to be an important factor. Structural and magnetic characteristics of CoPtCr-SiO_2 recording layers are also strongly affected by the grain size and the surface structure of intermediate layers.

Fig.1 Schematic diagram of Fuji Electric’s perpendicular recording medium

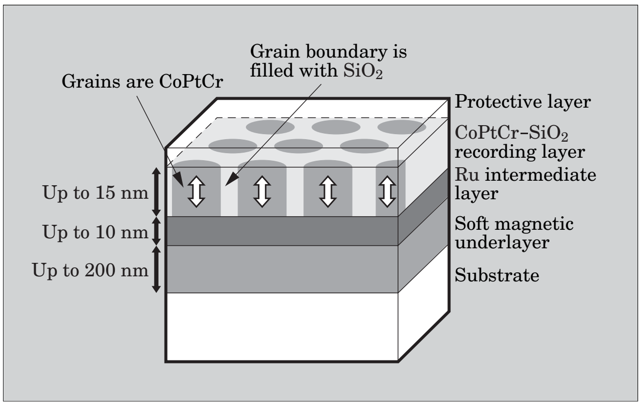

In this paper, we report on the characteristics of CoPtCr-SiO_2 media, and in particular, focus on the effect of the grain size and surface structure of Ru intermediate layers on the size and magnetic separation of grains in recording layers.

2. Control of the Grain Size in a Recording Layer

A finer grain of the recording layer does not necessarily contribute to further improvement of the read-write performance of media. Especially for granular magnetic layers with added SiO_2, grains tend to become too fine, which leads to the degradation of thermal stability, and in the worst case, to loss of magnetism at room temperature. Therefore, control of the grain size of Ru intermediate layers is important, as this determines the microstructure of the recording layer. An example is described below.

Figure 2 shows planar TEM (transmission electron microscopy) images of CoPtCr-SiO_2 magnetic layers for which the average grain sizes of Ru intermediate

Fig.2 Planar TEM images of the CoPtCr-SiO_2 magnetic layers. Ru grain sizes are (a) 9.9 nm and (b) 12.4 nm

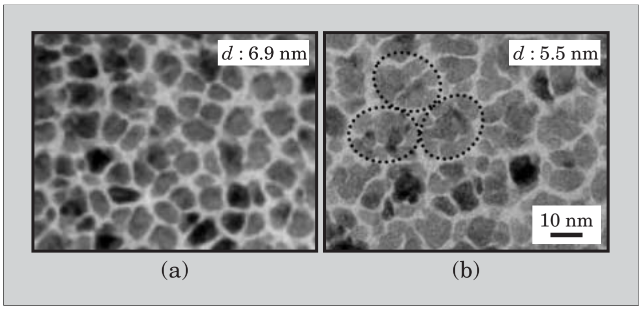

Table 1 Magnetic characteristics and read-write performance of samples (a) and (b)

Media	H_c (kOe)	R/W performance at 370 kfci		Decay at 30 kfci (% / decade)
		Normalized media noise	SN_mR (dB)	
(a)	6.39	52.9	12.4	1.5
(b)	4.98	90.8	8.98	0.5

layers are (a) 9.9 nm and (b) 12.4 nm, respectively. For the samples shown in Fig. 2, average CoPtCr grain sizes are (a) 6.9 nm and (b) 5.5 nm, respectively. It is interesting to note that the CoPtCr grain size of sample (b) is smaller than that of sample (a) despite its larger Ru grain size. We believe this is because grains in granular magnetic layers with added SiO_2 have a tendency to become too fine, and if the size of Ru grains exceed a particular threshold, multiple CoPtCr grains will grow on a single Ru grain. Dotted lines representing the size of Ru grains are shown in Fig. 2. It can be seen that multiple CoPtCr grains exist in each region surrounded by a dotted line. In contrast, CoPtCr grain growth achieves a one-to-one correspondence with Ru grains in sample (a). Table 1 shows the magnetic characteristics and read-write performance of samples (a) and (b). As shown in the table, sample (b) has poorer coercitivity (H_c), medium noise and SNR (signal-to-noise ratio) than sample (a), regardless of the fact that the CoPtCr grain size of sample (b) is smaller than that of sample (a). However, the decay (degradation rate of output signal) of sample (b) is smaller than that of sample (a), i.e. sample (b) is thermally more stable than sample (a). Judging from these results, it is believed that the magnetic reversal unit of sample (b) is larger than that of sample (a), i.e. grains of sample (b) are more strongly coupled than those of sample (a), despite the smaller CoPtCr grain size of sample (b). On the other hand, sample (a) has looser intergranular magnetic interaction despite its larger CoPtCr grain size.

As described above, control of the Ru grain size is important for realizing a one-to-one correspondence in the growth of Ru and CoPtCr grains, which leads to the control of CoPtCr grain size and reduction of intergranular magnetic interaction.

3. Control of Magnetic Cluster Size

3.1 Magnetic cluster size

It is known that magnetization reversal of a recording medium occurs in units of magnetically coupled grains rather than on a per-grain basis. Intergranular magnetic interaction is thought to generate such granular units, which are called magnetic clusters. Magnetic cluster size ($D_{cluster}$) can be measured using magnetic force microscopy (MFM), and it is also known that $D_{cluster}$ calculated from a MFM image is useful to analyze the origin of media noise[4]. For example, it has been reported that media noise in longitudinal media increases with increasing saturation magnetization of the recording layer even in the absence of exchange coupling because the increase of $D_{cluster}$ due to the magnetostatic interaction enhances the zigzag transition[5]. Transition noise is also reported to be the dominant source of noise in perpendicular media[6]. Accordingly, it is necessary for both longitudinal media and perpendicular media to reduce the zigzag transition, i.e. reduce $D_{cluster}$, in order to reduce media noise.

3.2 Evaluation of $D_{cluster}$

As stated above, MFM and image processing techniques are often used for the evaluation of $D_{cluster}$. We also have previously used that method and obtained the result that reducing $D_{cluster}$ is an effective means to increase both bit and track densities[7]. Here we are concerned with another evaluation method in which $D_{cluster}$ is estimated using the M-H loop slope parameter α (=$(dM/dH)_{H=Hc}$)[8]. For a perpendicular magnetic film, it is known that when perpendicular magnetic columns with no exchange interaction rotate coherently, α can be computed from the demagnetization factor (using cgs units) as:

$$\alpha = 4\pi / (N_z^f - N_z) \quad (1)$$

where N_z^f is the perpendicular-to-film directional demagnetization factor of the film, and N_z is that of the magnetization reversal unit. The demagnetization factor is a constant and is only dependent on the shape of the magnet. For example, the demagnetization factor equals 0 if the shape of the magnet is an infinitely long fine wire in the magnetization direction, and equals 4π if the shape of the magnet is an infinitely large thin sheet. For the recording layer of perpendicular media, N_z^f of equation (1) can be considered to be 4π because the film thickness is very thin compared to the dimensions of the film surface. Then, N_z can be obtained by determining α, and $D_{cluster}$ can be calculated according to the film thickness and N_z assuming that the magnetic clusters have cylindrical shapes of which demagnetization factors have been experimentally obtained as a function of the major-to-minor axis ratio. Based on that same assumption, an α-film thickness curve can be calculated to give a

Fig.3 Planar TEM images of samples using processes A and B for the deposition of Ru intermediate layers

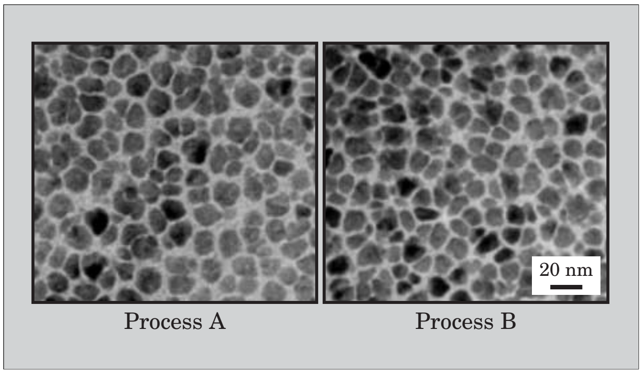

Table 2 Magnetic properties and read-write performance for process A and B media

Process	K_u (erg/cm^3)	H_c (kOe)	R/W performance at 300 kfci	
			Normalized media noise	SN_mR (dB)
A	3.55×10^6	2.09	47.5	12.6
B	3.21×10^6	2.04	29.6	17.3

certain $D_{cluster}$ value.

In the experiments, α-film thickness curves calculated from certain $D_{cluster}$ values were fitted to measured α values of different recording layer thicknesses, and $D_{cluster}$ was determined from the most suitable curve.

3.3 Influence of the Ru deposition process

Planar TEM images of the samples using processes A and B for the deposition of Ru intermediate layers are shown in Fig. 3. Moreover, magnetic properties and read-write performance at the linear density of 300 kfci are given in Table 2. The recording layer thickness of these samples is 8 nm. Although not shown in detail, the surface structure of Ru was varied when using process A or B. There is no marked difference in appearance such as grain size or segregation state (see Fig. 3), nor in magnetic properties such as K_u or H_c (see Table 2). However, in comparing the read-write performance shown in Table 2, the process B media has 40 % less media noise and 4.7 dB higher SNR than the process A media. In this case, the read-write performance differs substantially for each sample but the reason for this cannot be ascribed to the microstructure or magnetic properties. Therefore, $D_{cluster}$ was evaluated to examine the cause of differences in the read-write performance.

Figure 4 shows the recording layer thickness dependence of α, in which circles and squares indicate experimental values. The solid and dotted lines in Fig. 4 are lines that have been fitted to experimental data using the previously described method. These lines fit closely to the experimental data, and $D_{cluster}$ values of process A and B media are estimated to be 35 and 17nm, respectively. Furthermore, although the results are not shown in this paper, the $D_{cluster}$ of process A media is found to be larger in the initial layer where the effect of the surface of the Ru intermediate layer on the recording layer is especially large.

Fig.4 Recording layer thickness dependence of α

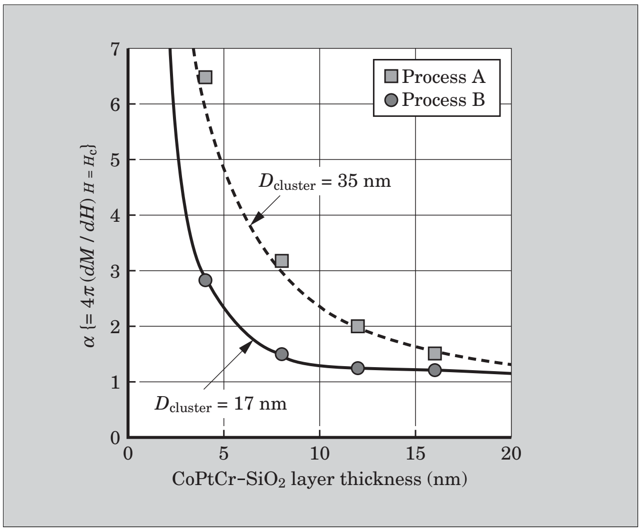

As described above, it is found that the surface structure of the Ru intermediate layer is reflected in $D_{cluster}$ and read-write performance. Further optimization of the depositing conditions of Ru is considered to be an effective means for decreasing $D_{cluster}$ and improving media performance.

4. Conclusion

A method for controlling the structure of CoPtCr-SiO_2 recording film was reported, focusing on the effect of the grain size and surface structure of Ru intermediate layers. Especially in the case of a larger $D_{cluster}$ in the initial growth region of CoPtCr-SiO_2 that results in poorer read-write performance, it is pointed out that in addition to TEM or commonly used magnetometer based methods, a more detailed analytical method such as $D_{cluster}$ analysis is needed to identify the cause. In perpendicular recording media, recording layer properties are affected by many factors such as surface roughness of the substrate and soft magnetic underlayer, and deposition conditions of the recording layer itself. We plan to optimize those conditions to realize perpendicular recording at high densities above 200 Gbits/in^2 and also to reduce costs for commercial application at the earliest feasible time.

In the near future, we expect perpendicular recording systems to be employed not only in computers, but also in audio-visual applications, which require compact size and large capacity.

References

(1) Iwasaki, S.; Takemura, K. An analysis for the circular

mode magnetization in short wave length recording. IEEE Trans. Magn. vol. Mag-11, 1975, p.1173.
(2) Oikawa, S. et al. High Performance CoPtCrO Single Layered Perpendicular Media with No Recording Demagnetization. IEEE Trans. Magn. vol. 36, 2000, p.2393.
(3) Oikawa, T. et al. Microstructure and Magnetic Properties of CoPtCr-SiO_2 Perpendicular Recording Media. IEEE Trans. Magn. vol. 38, 2002, p.1976.
(4) Takahashi, M. et al. The Dependence of Media Noise on the Magnetic Cluster Size for Co Based Thin Film Media Fabricated under Ultra Clean Sputtering Process. IEEE Trans. Magn. vol. 34, 1998, p.1573.
(5) Chen, J. et al. Magnetic cluster and medium noise in CoCrTa/Cr longitudinal film media studied by magnetic force microscopy, J. Appl. Phys. vol. 85, 1999, p.1037.
(6) Miura, K. Proc. SRC 12th Technical Review Meeting, 2001, p.185.
(7) Takenoiri, S. et al. Magnetic Properties, Magnetic Cluster Size and Read-write Performance of CoPtCr-SiO_2 Perpendicular Recording Media. IEEE Trans. Magn. vol.39, 2003, p.2279.
(8) Honda, N. et al. Simulation Analysis for Ring Head Recording on Single-layered Perpendicular Recording Media. IEICE Trans. Electron. vol. E82-C, 12, 1999, p.2184.

Wireless Link Design for Contactless Smart Cards

Shiro Kondo
Tatsuyuki Shikura

1. Introduction

Fuji Electric has a history of working to develop short-range wireless communications which can operate with relatively low power such as specified low power radios and high-frequency equipment. Although these wireless devices are convenient because wireless licenses are not required, their use often leads to problems since adequate link quality is not guaranteed. In response to this problem, through research into the concept of a wireless system that takes into consideration the characteristics of wireless channels and information, Fuji Electric has succeeded in the practical use of wireless devices. Contactless smart cards have experienced an especially dramatic increase in wireless applications in recent years, and various reader-writer (RW) devices have been commercialized for use with Sony Corporation's FeliCa card which exhibits the excellent characteristics of high speed and high security.

This paper focuses on the wireless communications technologies of contactless smart cards and describes relevant technical points and Fuji Electric's activities in this field.

Fig.1 Wireless link model

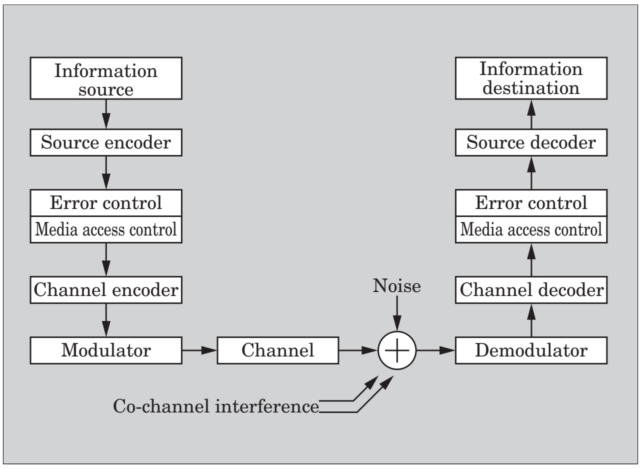

2. Wireless Link Design for Contactless Smart Card Systems

2.1 Wireless link model

The portion of a wireless system that transmits digitized information from an information source to an information destination can generally be modeled as shown in Fig. 1. Many various methods have been proposed for the modulator, encoder and other systems of Fig. 1, and this is a consequence of supporting the many various properties of information to be transmit and characteristics of the communication channels.

A contactless smart card system handles information in the form of digital data, typically electronic money information, and the handling of this information must be totally error-free. Moreover, the communication range d is on the order of ten and several of centimeters, the carrier frequency wavelength is approximately 2.2 m (frequency of 13.56 MHz) and the relationship of $d < \lambda/2\pi$ must be maintained. This is

Fig.2 Operating principles

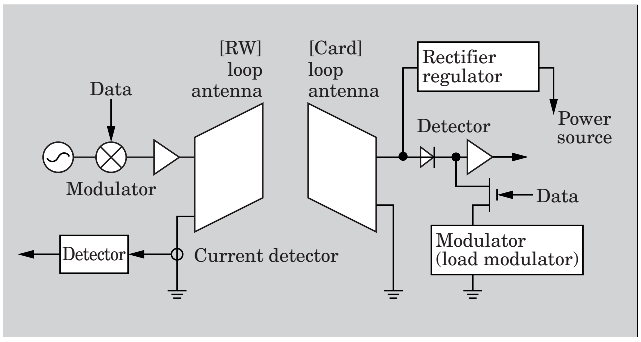

Table 1 Specification of physical and data link layers

Item		Specification
Carrier frequency		13.56 MHz
Modulation method	RW → card	ASK (approx. 10 % modulation)
	Card → RW	LM (load modulation)
Data rate		211.875 kbits/s
Bit coding		Manchester
Error control		FCS-based error detection + ARQ (auto repeat request)

because the communication uses induction coupling, and due to various factors, fluctuation in one characteristic (for example, antenna impedance), will affect the performance of the system.

2.2 Principles of RW operation

Figure 2 shows principles of RW device operation. First of all, since the smart card does not have its own power supply, the RW supplies power to the card while communicating with it. While the RW and card loop antenna (card antenna) are in an inductively coupled state, the RW supplies power to the card via a 13.56 MHz carrier wave. At the same time, in the case where data is to be transmitted from the RW to the card, the RW transmits approximately 10 % modulated ASK (amplitude shift keying) signal. The card detects that signal and converts it into data. Conversely, in the case where data is to be transmitted from the card to the RW, while the card is receiving continuous wave signals from the RW, the card switches its own impedance of the antenna in accordance with data stream to be transmitted. The RW detects this load switching as fluctuations in the voltage and current of its own loop antenna (RW antenna), and then demodulates the data.

Main specifications of the FeliCa physical layer and data link layer are listed in Table 1.

3. Challenges for Contactless Smart Card Communications

3.1 Required link quality and error control

The link quality and error control to realize error-free operation are described below. Strong error correcting techniques have been commonly applied in recent years in order to achieve error-free operation, however, since a contactless smart card system has a packet length of several hundred bits, the effectiveness of error correction is thought to be rather limited when there are only random errors.

Therefore, if a relatively good bit error rate can be guaranteed, a method that combines a low redundancy error correcting code with an auto-repeat request (ARQ) function is believed to be more suitable than the use of an error correcting code having poor encoding efficiency. In accordance with this belief, FeliCa uses ARQs to remedy errors.

With this method, however, it is known that if the bit error rate of the link deteriorates, then the number of ARQs will increase and the packet success rate will suddenly drop. In the case where the packet length is 256 bits and ARQs are implemented twice, a link is required to have a bit error rate of approximately 10^{-5} or better in order to achieve a packet error rate of 10^{-8}. On the other hand, in order to obtain a bit error rate of 10^{-5} with ASK asynchronous detection, a SN ratio of approximately 15 dB is required, and the RW should be able to guarantee these target values.

3.2 Challenges

The key to realizing the targeted bit error rates as described above is the response to fluctuations in impedance and other characteristics that have been mentioned in section 2, and specifically the response to fluctuations in card characteristics and suitability to the RW installation environment. Although called a "contactless smart card," its shape leverages advantages not necessarily associated with cards and some commercialized devices feature a chip embedded in a wristband or watch. Moreover, the embedding of chips into cell phones is about to come into widespread practice. Because there are various media characteristics, Fuji Electric's RW devices are targeting general-purpose applications and the guarantee of interconnectivity is extremely important.

In an actual system, the design challenge is to provide the capabilities to simultaneously distinguish multiple cards and to suppress co-channel interference from multiple RW devices. The abovementioned challenges are summarized below.

(1) Support of various types of media and suitability with the surrounding environment
(2) Simultaneous recognition of multiple cards (anti-collision mechanism)
(3) Suppression of co-channel interference from multiple RW devices

Efforts to overcome these challenges are described in detail below.

4. Technologies for Supporting Various Types of Media and Maintaining Suitability with the Surrounding Environment

Figure 3 shows one example of the influence of media characteristics on communications. The relationship between the card-to-RW distance and the strength of the signal voltage from the card to the RW device is shown with card resonant frequency f_c varied as a parameter. Several different card resonant frequencies are shown, and as can be seen, the characteristics differ dramatically when f_c is different.

Fig.3 Relation between communication range and signal voltage

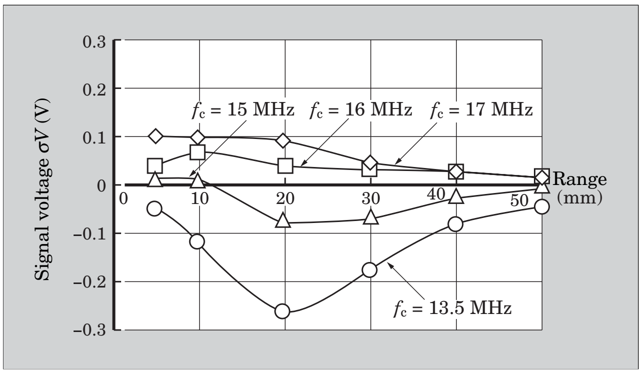

Moreover, in examining the characteristics for the case where f_c = 15 MHz, it can be seen that the signal voltage crosses zero at a distance of approximately 10 mm. This is a dead point (null point) and indicates that communication is not possible even though the card is within the communication range of the RW device.

Figure 4 is an analysis of the effect on the impedance of the RW antenna when that antenna is installed in close proximity to a metal plate. It is understood that the flow of eddy currents in the metal plate cause the self-inductance component to decrease and the resonant frequency to shift toward a higher frequency.

As described above, media characteristics in the surrounding environment have a large effect on the communication performance. Therefore, when installing a RW device on the front of an automated vending machine, for example, the parameters must be optimized for those installation conditions. To increase the efficiency of the development and design work, Fuji Electric has developed a hybrid analysis technique as shown in Fig. 5 that combines electromagnetic analysis and circuit analysis. Specifically, a high frequency electromagnetic analysis program capable of analyzing both wire antennas and planar antennas is used to analyze the self and mutual inductance, resistance and other constants of the RW device and card antenna with consideration of the effects from metal and the like. Meanwhile, the abovementioned constants are imported into a circuit analysis where RW characteristics such as the communication range and matching impedance are analyzed. As a result, the characteristics can be predicted and the shape of the RW antenna can be optimized prior to building a prototype.

These technologies have been applied to develop the RW device shown in external view in Fig. 6. Figure 7 shows the relationship between the communication range and card frequency for this RW device. The prototype card shown in the figure is for evalua-

Fig.4 Influence of a metal plate

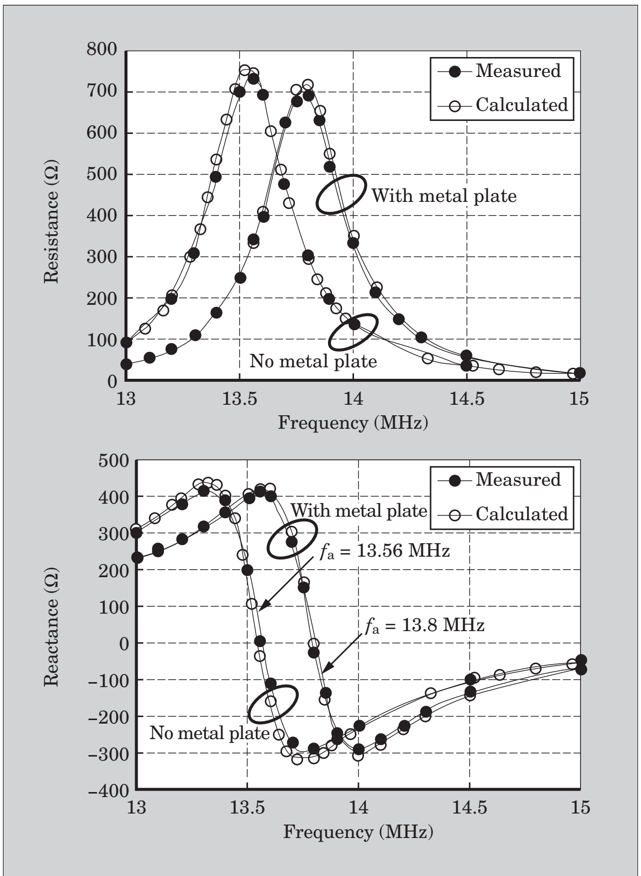

Fig.5 Hybrid analysis technique

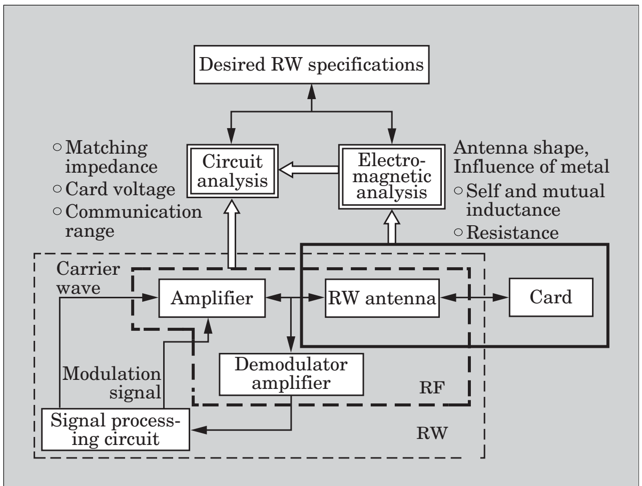

Fig.6 External view of RW device

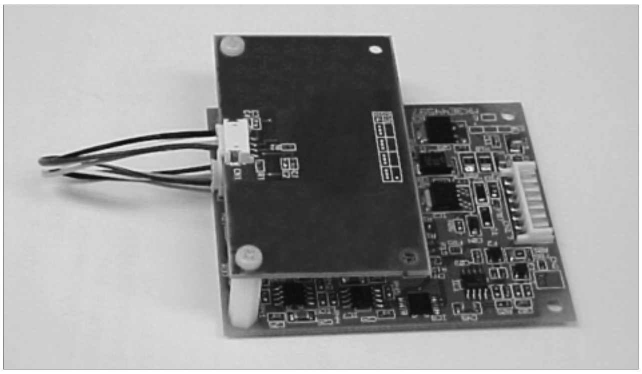

Fig.7 RW communication range

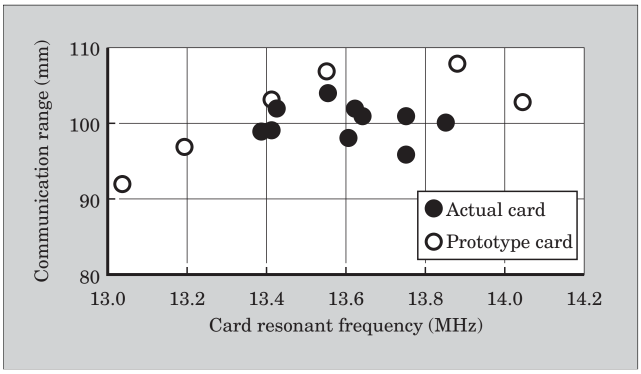

tion purposes and is configured from a card antenna and chip that enable the card frequency to be varied. A communication range of 90 mm or more was realized over a wide range of card frequencies. In addition, constants were optimized to achieve communication without any dead points and the design has minimized the number of locations for adjustment so that when installed in another machine, adjustments may be performed easily according to that installation environment.

5. Simultaneous Recognition of Multiple Cards

In contactless smart card communication, the capability to simultaneously recognize multiple cards is essential and there are basically two techniques which provide this capability.

The first solution is an anti-collision technique in which the card ID is acquired by a slotted ALOHA procedure.

The second technique solves the problem of the large fluctuation in characteristics caused by mutual coupling that occurs when there is overlap from multiple cards. Accordingly, schemes have been proposed for f_c and the antenna known as an anti-collision card, and the optimal RW design that supports these characteristics can be realized by applying the analysis techniques described in section 4.

6. Inter-RW Interference

Figure 8 shows an example of a practical application in which a contactless wristband is used to control the opening and closing of locks on locker doors. Because a lot of RW devices are installed in close proximity to one another, there is the possibility that the electromagnetic field generated by one RW device may effect to other RW devices.

Figure 9 shows a model of the interference between RW devices. Here, the effect of inter-RW interference is greatest when one RW device is receiving a signal from a card while adjacent RWs are simultaneously generating downlink signals. The downlink signals from an RW device are either unmodulated or ASK modulated.

In the case of an unmodulated signal, if the desired channel and interference channel have different carrier frequencies, cross modulation will occur at the detector circuit and the phenomenon of beating will appear. In an actual RW device, however, the carrier frequency tolerance is suppressed to approximately 50 ppm and therefore the beat frequency will only be several hundred Hz at most. Moreover, by encoding the bits in a Manchester encoding scheme, the receiver will cut low frequencies and unmodulated signals will not actually be a significant problem.

On the other hand, in the case of ASK modulated signals, the overlap between the frequency bandwidth

Fig.8 Locker system

Fig.9 Inter-RW interference model

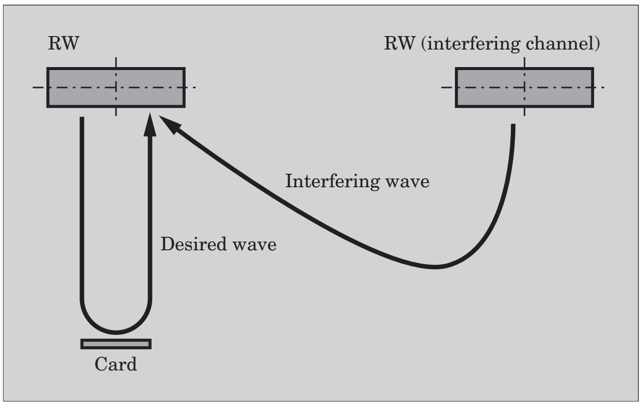

of the interference signal and the frequency bandwidth of the desired wave is potentially troublesome. In this case, no matter how much the signal output level is raised to improve its SN ratio, the bit error rate will show almost no improvement and therefore it will be necessary to implement such measures as redesigning the RW device in order to lower the interference power, employing controls to avoid the simultaneous operation of adjacent RW devices and so on. However, these measures will have the undesirable effect of degrading the responsiveness to cards, and therefore in the above example, the design has optimized to meet these challenges.

7. Conclusion

Focusing on the wireless communication of contactless smart cards which are soon be put into practical applications, this paper has presented key technologies for the interconnectivity of cards and RW devices and for application to systems. Fuji Electric will continue to improve these RW technologies and to promote further development of contactless smart cards.

Recent Optimization Techniques and Applications to Customer Solutions

Shinji Kitagawa
Michio Takenaka
Yoshikazu Fukuyama

1. Introduction

Companies operate by setting goals in various business fields, and then taking action to achieve those goals. Optimization techniques are one way to obtain operation (decision making) that will, to the extent possible, approach goals that have been set in response to a given problem. As a result, solutions such as designs for minimal operating cost, optimal product quality, smallest device size and the like can be realized.

The development of optimization techniques began during World War II, when they were used to optimize the trajectory of missiles. Subsequently, mathematical programming has been developed to realize optimization through the application of mathematical techniques. Additionally, the optimization technique of meta-heuristics (MH), which imitates physical phenomena and the evolution of living organisms, has been developed since the 1970s. Furthermore, Fuji Electric has begun working to develop an optimization technique that is superior to conventional meta-heuristics. In the past, new optimization techniques had been developed in each era in order to realize customer solutions. But now, those optimization techniques are dated and new solutions are being realized.

This paper introduces recent optimization techniques and their application to customer solutions.

2. Recent Optimization Techniques

2.1 Problems with conventional decision-making techniques and characteristics of requested techniques

When making a decision in order to achieve a certain goal, mathematical optimization techniques such as mathematical programming have been utilized in cases where the target problem can be expressed as a mathematical equation (conventional technique 1 in Fig. 1). On the other hand, if the target problem cannot be expressed in a mathematical equation, neural networks, fuzzy logic, expert systems and other decision-making techniques have been utilized (conventional technique 2 in Fig. 1). In cases where the mathematical expression is only an approximation, practical use of conventional technique 1 was potentially difficult. The problem with conventional technique 2 is the difficulty in guaranteeing the generation of good quality solutions for cases that have not been verified. Moreover, analytical calculation for each target problem is often possible with a general-purpose program (such as a finite element package, for example). However, as shown in Fig. 1, with conventional technique 1, it is not possible to isolate the target problem from the optimization program, and it was difficult to coordinate use with an independent general-purpose program in order to analyze the target problem.

Therefore, in consideration of crude onsite operating constraints such as the constraint of only being capable of expressing if-then rules, and in consideration of other factors such as the coordination with an independent general-purpose program, a technique that can obtain good solutions — even in cases that have not been verified — is required. As a recent optimization technique capable of responding to these types of needs, Fuji Electric is researching and devel-

Fig.1 Conventional decision making techniques and recent optimization techniques

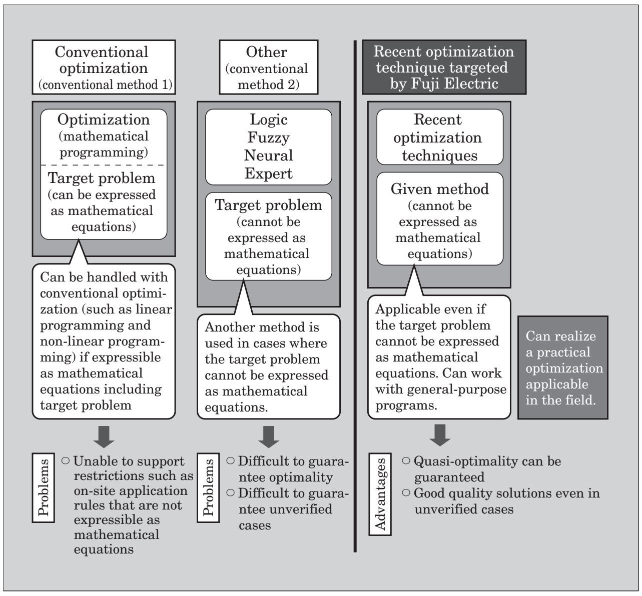

oping a new optimization technique that uses meta-heuristics and the stability theory for nonlinear systems as described below.

2.2 Meta-heuristics

Meta-heuristics is a technique that uses simulations of the behaviors involved in physical phenomena and living organisms to realize a general-purpose optimization search framework that does not depend on the target problem.

Various meta-heuristic techniques exist, including genetic algorithms (GA), simulated annealing (SA), tabu search (TS) and particle swarm optimization (PSO) (see Table 1).

GA uses chromosomes to express a problem and searches for a solution with alternations of generations using natural selection and genetic operations such as cross-over and mutation. SA searches for solutions by modeling the gradual decrease in molecular vibration when liquid steel is cooled and solidified into a solid state and a minimum energy state is reached. TS realizes effective searches by searching for only new solutions and prohibiting (tabu) a return to any solutions that had been searched for previously. PSO searches for solutions by modeling the condition in which a swarm, such as a flock of migrating birds, behaves skillfully as a group or a decision making process in which personal information is shared skillfully among a group. Here, the mixed-integer nonlinear optimization problem for PSO is a problem of finding the combination of optimal values for state variables that contain both discrete variables (such as the tap values of a transformer, for example) and continuous values (the output of an electric power generator, for example). A typical optimization problem considers both discrete and continuous variables, and often becomes a mixed-integer nonlinear optimization problem. Fuji Electric has successfully applied PSO for the first time in the world in the fields of power and energy.

The recent PSO technique, which is applicable to various fields, is summarized below. PSO was developed in 1995 at Purdue University by Professor Eberhart et al. PSO is a solution search technique in which the particle has become a swarm. There are two techniques behind the development of PSO. The first is the technique of modeling the behavior of a swarm, such as a herd of animals, and the second is cognitive psychology. The behavior of a flock of migrating birds can be expressed simply as a combination of vectors, i.e. a vector pointing toward the center of the flock, a vector that maintains a constant distance with neighboring birds, and a vector pointing in the direction of the flock's flight path. It is known that the behavior of the flock can be modeled with extreme accuracy by adding an appropriate random number to these three vectors. Moreover, in the field of cognitive psychology, it is known that decisions are made based on a person's own experience and the experiences of people. Professor Eberhart developed PSO, which is more efficient for searching than conventional meta-heuristics, by preparing multiple solution search points (corresponding to multiple birds), and as shown in Equation (1), searching for a solution based on a personal best

Table 1 Comparison of meta-heuristic techniques

	GA	SA	TS	PSO	Recent optimization technique using stability theory for nonlinear systems
Development period	1970s	1983	1989	1995	2003
Target problem	Combinatorial optimization problem	Combinatorial optimization problem	Combinatorial optimization problem	Continuous optimization problem , Mixed-integer nonlinear optimization problem	Combinatorial optimization problem, Continuous optimization problem, Mixed-integer nonlinear optimization problem
State variable	Discrete variable	Discrete variable	Discrete variable	Continuous variable, Discrete variable	Continuous variable, Discrete variable
No. of search points	Multi-point search	Single point search	Single point search	Multi-point search	Single point search
Solution guarantee	Guaranteed that all solutions will be in a favorable direction	Guaranteed that global minimum will be obtained	No mathematical guarantee	Trial mathematical analysis of search behavior is underway.	Able to guarantee with a search method based on mathematical theory (logic is being formulated)
Run time	Medium	Long	Short	Short	Medium
Features	In recent years, application efficacy for multi-objective optimization problems has been under review.	A good quality solution can be obtained, but it will require a long amount of time.	Good quality solutions can be obtained for combinatorial optimization problems in a shorter amount of time than with GA or SA	Good quality solutions can be obtained within a short amount of time for mixed-integer nonlinear optimization problems, for which solutions were difficult to obtain with conventional methods.	The most efficient and accurate solution can be obtained for large-scale problems.

(Pbest) point (corresponding to one's personal experience) having the best evaluation among individual search points and a group best (Gbest) point (corresponding to experience that includes other people's experiences) having the best evaluation among the swarm of search points, while changing the direction of the search in the direction of the present search direction composite vector.

Next search direction = Present search direction
+ Pbest direction + Gbest direction ················ (1)

In actuality, a weighting factor (function) is applied to each term on the right side of the equation, and the present search direction is initially set to a random value. Consequently, in the search space, multiple birds (search points) search for the optimal solution while exchanging information of favorably evaluated search points (Fig. 2).

Fuji Electric has added improvements to this recent PSO technology to realize solutions that use a constricted factor approach, hybrid PSO, adaptive PSO, etc.

2.3 New optimization techniques using stability theory for non-linear systems

Meta-heuristics has an advantage in that a good quality solution can be obtained even in cases when the target problem cannot be expressed as an equation or it is necessary to use general-purpose software. However, for practical purposes, the probability of producing a good quality solution decreases for large-scale problems. Rather than optimization within a small range, as is often said, end users require "total optimization" over a broad range that may expand from one building to an entire factory and then to an entire production operation. In the future it will be necessary to deal with even larger scale problems. Moreover, since techniques such as GA, SA and PSO are stochastic methods, there is no guarantee that a good quality solution will always be obtained, and moreover, a different solution may be obtained each time. If the same solution were to be obtained each time, the degree of freedom would decrease and the probability of obtaining a good solution would also decrease. For this reason, it is necessary to carefully tune a search for the purpose of practical utility. Fuji Electric is developing a new optimization method based on stability theory for nonlinear systems that will compensate for these types of deficiencies in meta-heuristics and will always yield a good quality solution for large-scale problems (Table 1). An overview of this method is described below.

Mathematical programming has been developed as a way to find local minima by calculating the slope of the objective function of each search point in an optimization process (① in Fig. 3). With this method, however, it is not possible to escape from a local minimum to find the global minimum located in another valley (② in Fig. 3). In order to overcome this disadvantage of mathematical programming, meta-heuristics were developed as a method for escaping from local minima by imitating the alternation of generations of living organisms and the behavior of swarms.

Here, in looking at the shape of the objective function in slightly greater detail, it can be seen that after reaching a local minimum, traveling through the lowest part of a mountain ridge is an effective way to reach the next valley. Similarly, once a local minimum has been obtained, the surrounding local minima can

Fig.2 Concept of particle swarm optimization

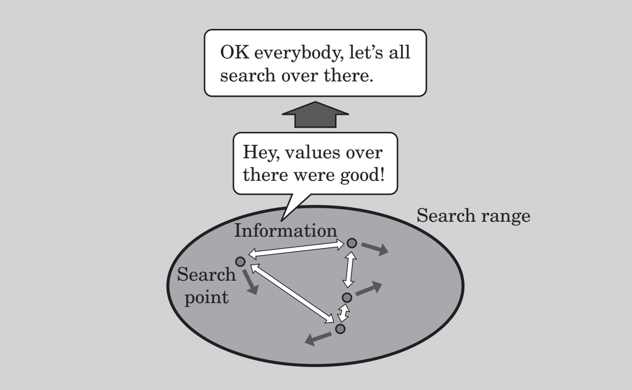

Fig.3 Concept of the escape from local minima

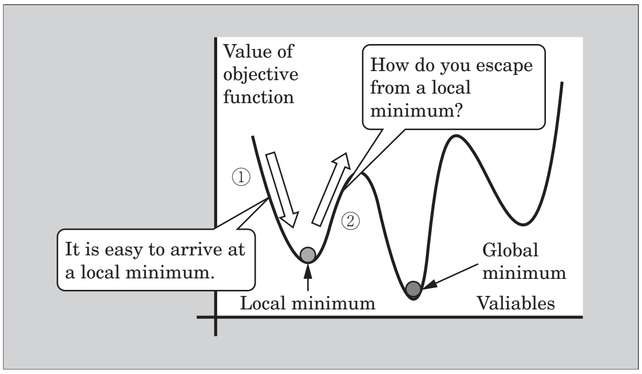

Fig.4 Efficient search method for local minima

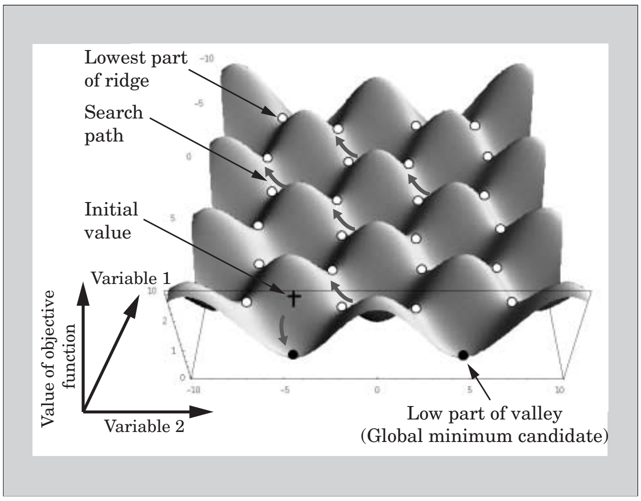

be obtained in a minimum amount of time by repeatedly traveling through the lowest part of mountain ridges to reach the local minima in neighboring valleys (Fig. 4). The optimal solution can be found as the best solution among local minima obtained within a given amount of time (solution closest to the global minimum). This type of method was proposed by Professor Chiang et al. of Cornell University, and has the disadvantage of requiring considerable run time.

Improving on this method, Fuji Electric is developing a method that uses continuation methods and eigenvalue analysis to quickly find the lowest point on a ridge and then find the local minima within a short amount of time. It has been verified that use of this method enables the global minimum to be obtained within a short amount of time, even in the case of large-scale and complex objective functions. Although this method is still in its research phase, practical R&D is advancing toward the realization of applications in various fields.

3. Solutions Using Recent Optimization Techniques

Here, the sensor diagnostic function in the optimal operation of an energy plant is presented as an example of a solution that uses optimization techniques.

Figure 5 shows the system configuration of an energy plant optimal operation system. The sensor diagnostic function is executed at the stage before data is input to each function of the optimal operating system as a historical data management function. Sensor measurement data acquired via a LAN are automatically corrected for measurement errors, and if the correction amount is large, the sensor is specified as an "abnormally measuring sensor" and the operator is notified. The sensor diagnostic function basically consists of the following two functions.

3.1 Sensor measurement correction function

For practical use, even if the sensor information contains measurement errors, various functions of the optimal operation system must realize continuous operation and output appropriate results. In order to continuously output appropriate results, a sensor measurement correction function operates to automatically correct sensor measurement values such that the error between a sensor measurement value and the plant simulator calculation result is minimized. This problem can be formalized as the following optimization problem.

State variables:
: Plant simulator input values (various types of fuel, load values, etc.)

Objective function:
: Minimization of the error between measured and calculated values

In other words, the combination of plant simulator input values for which the value of the objective function is a minimum, is obtained, and the sensor measurement value is automatically corrected based on the plant simulator calculation results at that time. Realization of this function is based on PSO, which is one of the meta-heuristic techniques.

3.2 "Abnormally measuring sensor" specification function

In cases where the correction by the abovementioned function is large, this "abnormally measuring sensor" specification function specifies the sensor thought to be the cause of that abnormality. This problem can be formalized as the following combinatorial optimization problem.

State variables:
: Combination of normal measurement and abnormal measurement sensor states

Objective function:
: Minimization of the error between normal measurement values and calculated values, and maximization of the probability that a "normally measuring sensor" will exist

In other words, the error between a measured value from a "normally measuring sensor" and a plant simulator calculation result, the number of "normally measuring sensors" that exist, and the like, are judged

Fig.5 Optimal operation of an energy plant having a sensor diagnostic function

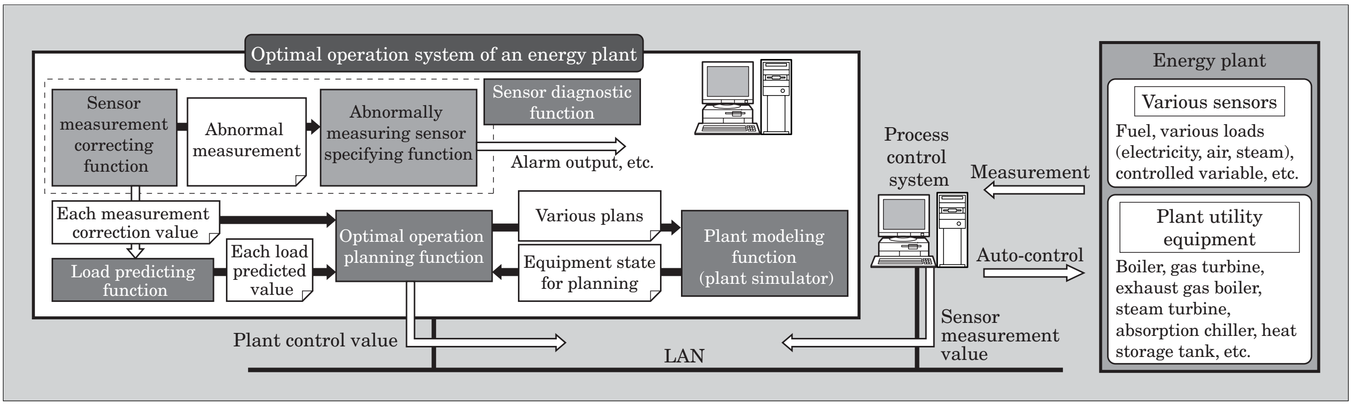

Fig.6 Examples of application areas of recent optimization techniques

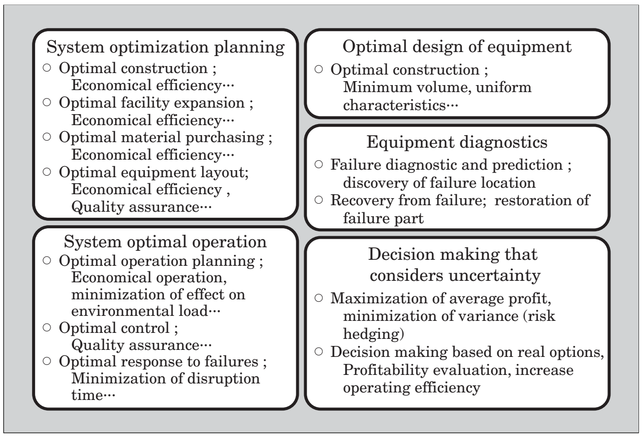

in a comprehensive manner, and the combination of sensor states that yield the best objective function value is obtained, and within that combination, sensors in an abnormal measuring state are specified as "abnormally measuring sensors." Moreover, using the same method as with the function of section 3.1, correction of the sensor measurement value based on the plant simulator calculation result may be realized at the same time as the best objective function value is obtained.

These functions utilize the results of an external program known as a plant simulator, and therefore, could not be realized with conventional mathematical programming. Moreover, these functions require meta-heuristic techniques and are realized based on PSO. With these types of functions, maintenance costs can be decreased by transferring from time-based maintenance (TBM) that performs regular maintenance to conditional-based maintenance (CBM) that performs maintenance on an as-needed basis. Fuji Electric is supplying the FeTOP and PowerCC as energy plant optimal operation tools that incorporate these types of sensor diagnostic functions.

Figure 6 lists examples of the application areas of these recent optimization techniques.

4. Conclusion

This paper has discussed recent optimization techniques being developed by Fuji Electric and presented examples of applications to solutions. In the future, Fuji Electric intends to advance optimization techniques further and to realize customer solutions.

References

(1) Fukuyama, Y. et al. Tutorial on Modern Heuristic Optimization Techniques with Applications to Power Systems Organized by K.Y.Lee and M. El-sharkawi. IEEE PES Winter Meeting. 2002.

(2) Fukuyama, Y. et al. A Method for Computing a Global Optimal Solution of Continuous Optimization Problem. Proc. of International Conference on Soft Computing and Intelligent Systems and International Symposium on Advanced Intelligent Systems (SCIS & ISIS 2004).

(3) Holland, J. Adaptation in Natural and Artificial Systems: An Introductory Analysis with Applications to Biology, Control, and Artificial Intelligence. Bradford Books. 1975.

(4) Krikpatrick, S. et al. Optimization by Simulated Annealing. Science. vol. 220, no. 4598, 1983, p.671-680.

(5) Glover, F. Tabu Search Part I. ORSA Journal of Computing. vol. 1, no. 3, 1989.

(6) Kennedy, J.; Eberhart, R. Particle Swarm Optimization. Proceedings of IEEE International Conference on Neutral Networks. vol. IV, 1995, p.1942-1948.

(7) Fukuyama, Y. et al. A Particle Swarm Optimization for Reactive Power and Voltage Control Considering Voltage Security Assessment. IEEE Trans. on Power Systems. vol. 15, no. 4, 2000.

(8) Fukuyam, Y. et al. A Hybrid Particle Swarm Optimization for Distribution State Estimation. IEEE Trans. on Power Systems, vol. 18, no. 1, 2003.

(9) Fukuyama, Y. et al. Particle Swarm Optimization for Optimal Operational Planning of a Cogeneration Plant. Proc. of Meta-heuristic International Conference (MIC2003).

(10) Chiang, H. D.; Chu,C. C. A Systematic Search Method for Obtaining Multiple Local Optimal Solutions of Nonlinear Programming Problems. IEEE Transactions on Circuits and Systems-I. vol. 43, no.2, 1996, p.99-109.

(11) Fukuyama,Y. et al. Particle Swarm Optimization for Optimal Operational Planning of a Cogeneration System. Proc. of IASTED modeling, Simulation, and Optimization (MSO2004) (to be appeared).

(12) Fukuyama, Y. et al. Optimal Operational Planning of a Cogeneration Plant Considering Load Forecasting Error. Proc. of International Conference on Soft Computing and Intelligent Systems and International Symposium on Advanced Intelligent Systems (SCIS & ISIS 2004).

High Efficiency Power Conversion Using a Matrix Converter

Jun-ichi Itoh
Akihiro Odaka
Ikuya Sato

1. Introduction

As demands for energy savings have increased in recent years, inverters are being used in a wider range of applications. Demands for lower cost, smaller size and higher efficiency will continue to further expand the range of inverter applications. However, as a trend toward eco-friendly products increases, some sort of measure is necessary to suppress the harmonics contained in the inverter input current.

Fuji Electric is developing a matrix converter capable of converting a input voltage directly into an arbitrary AC voltage, instead of converting that voltage into a DC voltage as inverters. This matrix converter has higher efficiency, smaller size, longer lifespan and fewer input current harmonics than inverters and has high potential for realizing the abovementioned demands. This paper presents Fuji Electric's matrix converter and the new technologies that enable its practical application.

2. Principles of the Matrix Converter

Figure 1 shows the circuit configurations of an inverter and a matrix converter. The inverter is a well-known device that converts an input AC voltage into a DC voltage by a rectifier, and then controls the semiconductor switch of a PWM inverter to convert the DC voltage into the desired AC voltage. A voltage smoothing capacitor is required in the DC link circuit, and an electrolytic capacitor is typically used for this purpose.

On the other hand, the matrix converter arranges semiconductor switches into a matrix configuration and controls them to convert an input AC voltage directly into the desired AC voltage. Since the input AC voltage is not converted to a DC voltage, there is no need for an energy storage device such an electrolytic capacitor. Bi-directional switches are needed as the semiconductor switches, since an AC voltage is impressed on it.

As can be seen in Fig. 1 (a), the inverter requires a charge-up circuit to suppress the inrush current that flows to the electrolytic capacitor connected to the DC link circuit. If a diode rectifier is used as the rectifier, a large amount of input current harmonics will be generated and therefore, a DC reactor (DCL) is inserted to reduce the current harmonics in the input current. In a conventional inverter, it is necessary to connect a braking unit to the DC link circuit in order to dissipate the regenerated power from the motor. A PWM rectifier was often used to reduce the input current harmonics and to realize motor regeneration. The matrix converter, on the other hand, is able to realize motor regeneration with almost no input current harmonics. In other words, a single converter unit is able to provide performance equivalent to that of a PWM rectifier and an inverter. Additionally, the charge-up circuit is unnecessary since the large electrolytic capacitor is not needed for the matrix converter. As a result, smaller size and longer lifespan can be achieved. In Fig. 2, a matrix converter system is compared to a conventional system that uses a PWM rectifier and an inverter. The conventional system

Fig.1 Inverter and matrix converter

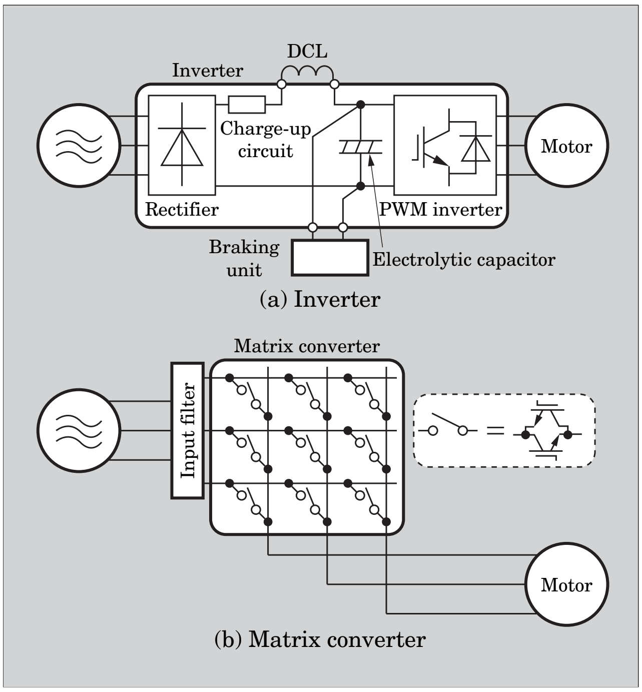

Fig.2 Comparison of the matrix converter with the conventional system

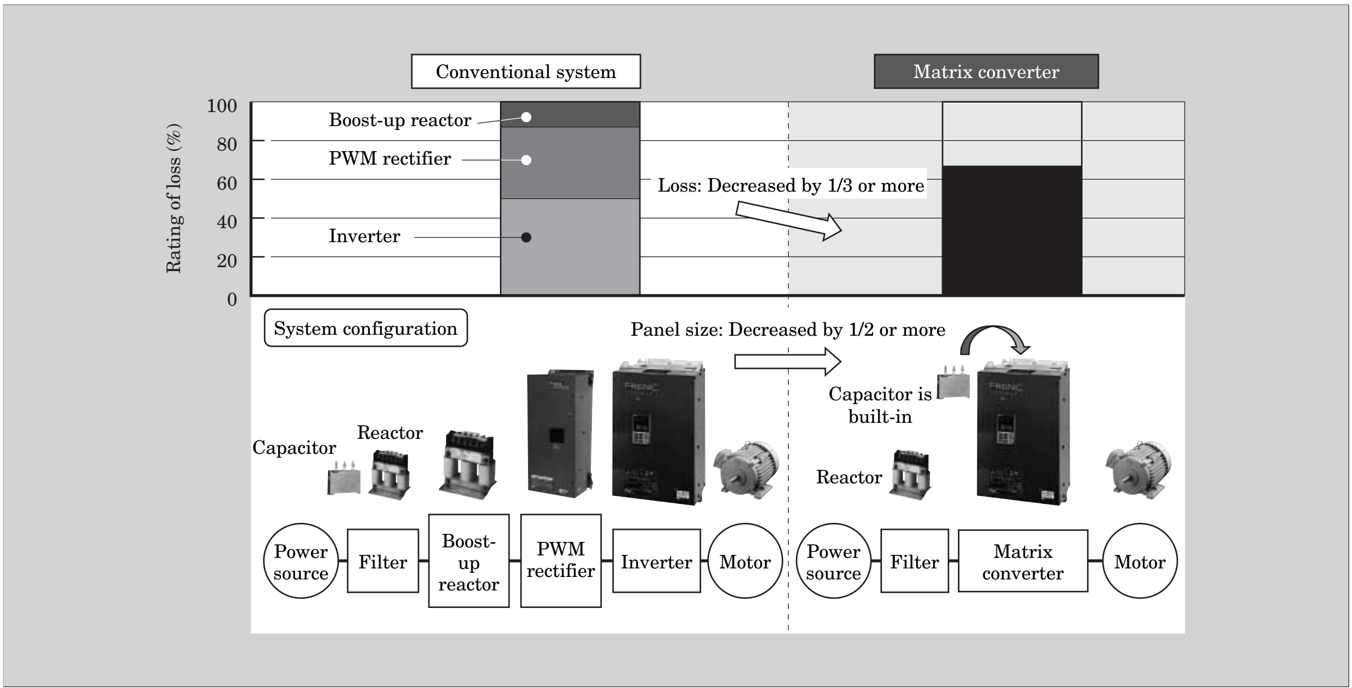

needs a filter capacitor, a filter reactor and a boost-up reactor in addition to a main unit. The matrix converter system, however, only needs a main unit and a filter reactor. Therefore, the configuration becomes simple and a panel size of the system can be reduced by 1/2 or more. In addition, since the matrix converter uses one-stage AC-AC direct conversion, a low loss system can be realized, achieving at least 1/3 lower loss than in the conventional system.

3. New Technologies for the Practical Application of Matrix Converters

The circuit configuration and operating principles of the matrix converter have been known for some time, but there are many problems in achieving practical application. The new technologies that solved these problems are introduced below.

3.1 Technology for realizing a reverse blocking IGBT

Table 1 shows the bi-directional switches that are used in matrix converter. An AC voltage is impressed on the bi-directional switches. Because conventional semiconductor switch such as IGBTs do not have reverse blocking capability, diodes for reverse blocking are needed as shown in Table 1 (a). The problem with this diode, however, was that it increased on-state loss and decreased efficiency.

In order to solve this problem, Fuji Electric is developing a new IGBT having reverse blocking capability (RB-IGBT). Under a reverse bias, the conventional IGBT generates a large leakage current because its depletion region extends to the dicing surface at the chip side, where severe strain exists after the mechanical dicing process. In the newly developed RB-IGBT, a deep isolation region is formed in the dicing area to prevent expansion of the side surface of the depletion region and to ensure the reverse-blocking capability. Recent advances in IGBT manufacturing technology have enabled the realization of this device. The RB-IGBT has the same basic structure as the conventional IGBT, and thus their characteristics are also similar. Moreover, the reverse recovery characteristic of the RB-IGBT is approximately the same as that of the conventional diode.

Table 1 Bi-directional switches

	(a)	(b)
Bi-directional switch 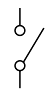	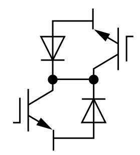	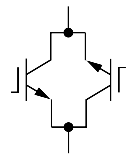
Number of devices	IGBT × 2, diode × 2	RB-IGBT × 2
On-state voltage	≈ 4 V	≈ 2 V

Figure 3 compares the loss of matrix converters with each of bi-directional switches shown in Table 1 (a) and 1 (b). By using the RB-IGBT, the on-state loss of a series-connected diode is eliminated and although the switching loss remains nearly the same, on-state loss can be reduced by approximately 30 %.

3.2 Protection technology

Figure 4 shows the commutation and protection circuit of the matrix converter. Commutation is the

Fig.3 Comparison of the matrix converter losses

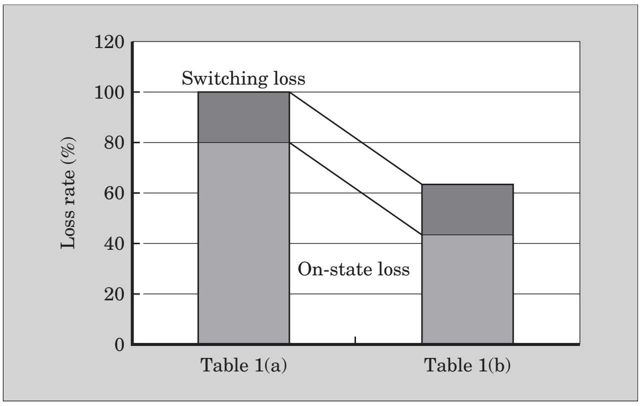

Fig.4 Commutation and protection circuit

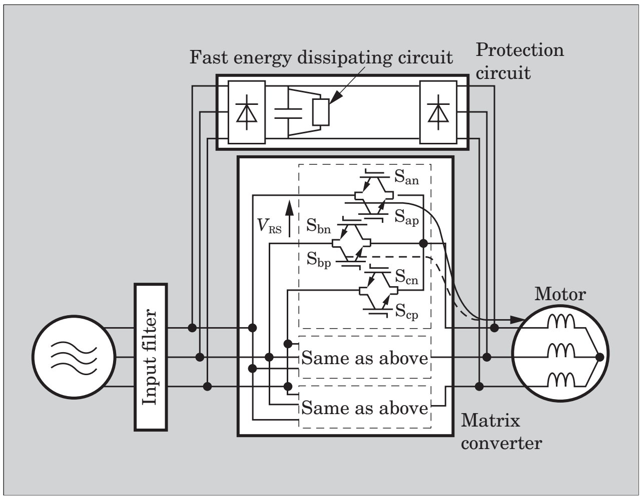

process wherein the current flowing to a switch S_a, for example, is transferred by turning on a switch S_b and turning off a switch S_a so as to transfer that current to switch S_b. The switch must be controlled, so that there is no short circuit and the load current is not interrupted. If the load current is interrupted, a large surge voltage is impressed upon the semiconductor switch and the switch is damaged.

Therefore, similar to the conventional PWM inverter, dead time is provided to prevent a short circuit condition and surge voltage generated during this dead time interval is absorbed by a protection circuit. As a result, loss increases and the protection circuit grows in size, as it requires a large electrolytic capacitor to absorb energy. This reduces the advantage of the matrix converter.

The commutation problem is solved by controlling the two RB-IGBTs that compose a bi-directional switch independently. In other words, by keeping a reverse-biased switch constantly in its on-state, the device is made to behave the same as the freewheeling diode in the conventional PWM inverter, and the load current is not interrupted. The forward-biased switch is turned-on and off with dead time and controlled similar to a conventional PWM inverter to prevent a

Fig.5 Control method for the matrix converter

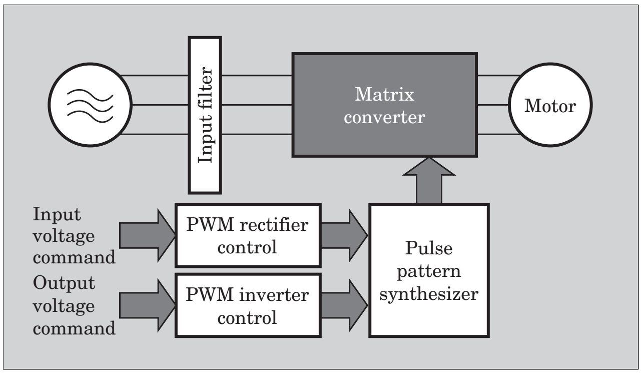

short circuit condition. For example, in Fig. 4, if $v_{RS} > 0$, S_{an} and S_{bp} are reverse biased and therefore are always turned-on, while S_{ap} and S_{bn} are turned-on and off with dead time. As a result, while short circuit conditions are being prevented, interruption of the load current is also prevented and the current is commutated safely. In addition, a protection circuit is necessary to protect the device from overcurrent and/or overvoltage. An electrolytic capacitor is generally used in the protection circuit to absorb energy stored in the load. However, using the electrolytic capacitor for the protection circuit reduces the advantage of the matrix converter. To overcome the problem, a new protection circuit is developed. The new protection circuit dissipates the load energy quickly without absorbing the energy to the capacitor. As a result, the electrolytic capacitor is not necessary.

3.3 Control technology

With the matrix converter, simultaneous control of the output voltage and input current is possible, but simultaneous and independent control is not easy to implement. The control method becomes complicated because switching one bi-directional switch in order to output a certain voltage causes the change of the input current condition. The higher speed, higher performance and lower cost of control devices in recent years, however, have made it possible to realize even complicated control with ease. In the conventional control method for a matrix converter, the pulse pattern for each bi-directional switch is calculated directly from the condition for obtaining the desired AC output voltage and the condition in which the input current becomes a sinusoidal wave. This control method is unique to the matrix converter and is capable of outputting various pulse patterns. However, since the pulse pattern is calculated directly, it is difficult to control the input current and the output voltage independently.

Then, a new control method was developed, and is shown in Fig. 5. This method is based on the virtual indirect control of a virtual PWM rectifier and a virtual PWM inverter. The matrix converter pulse pattern is obtained by synthesizing the pulse patterns of the

Fig.6 Principle of the virtual indirect control method

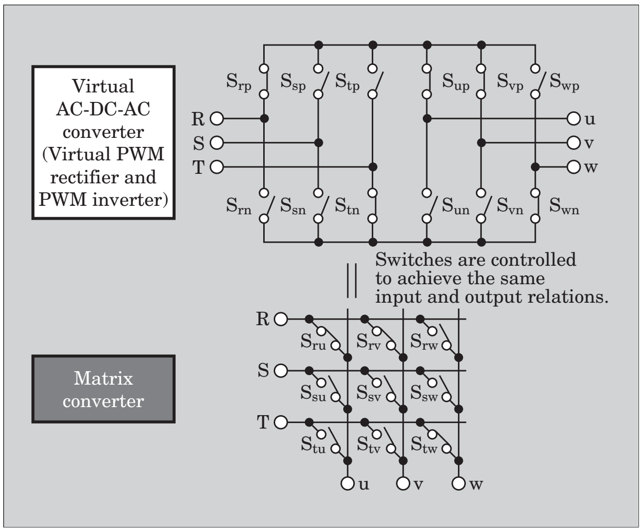

Fig.7 Input and output waveforms

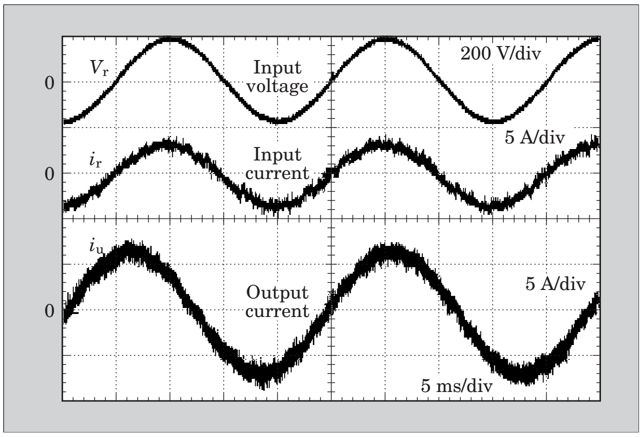

Fig.8 Input power factor and THD vs. load torque

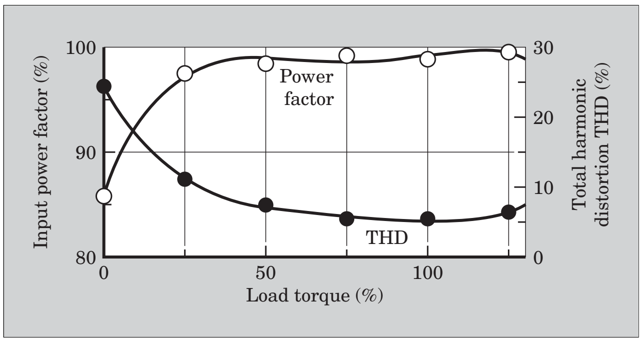

virtual PWM inverter and the virtual PWM rectifier. This method enables the input current and output voltage to be controlled independently. In addition, since this control method can be implemented as a direct extension of the control of the conventional PWM inverter, techniques developed in the past can be applied largely without change. The virtual indirect method controls the input current and output voltage, and as shown in Fig. 6, assumes a virtual converter comprised of a virtual PWM rectifier and a virtual

Fig.9 Acceleration and deceleration characteristics (100 r/min → 1,200 r/min → 100 r/min)

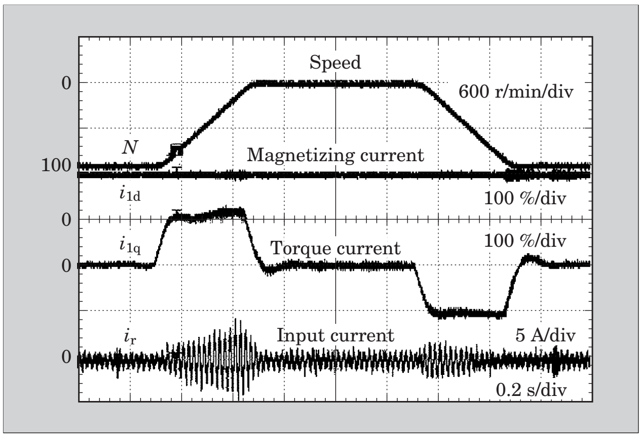

Fig.10 Impact load torque characteristic (0 % → 100 % → 0 %)

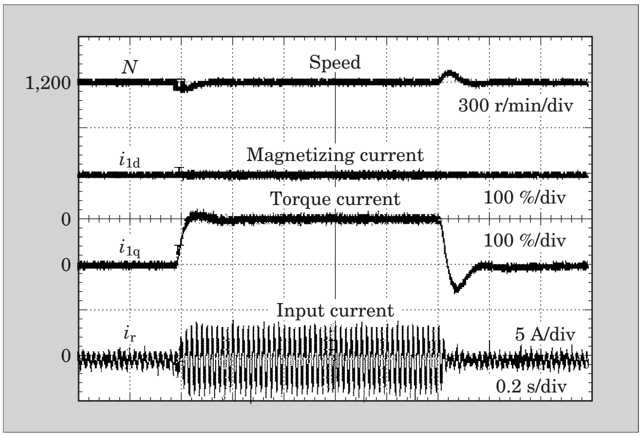

PWM inverter.

The virtual indirect control method is based upon the principle that states, "in a three-phase power converter, if the final input and output connection relations are made equal, then the input and output waveforms will not depend on circuit topologies." In Fig. 6 for example, if there exist intervals during which the virtual rectifier turns on switches S_{rp} and S_{tn}, and the virtual PWM inverter turns on switches S_{up}, S_{vp} and S_{wn}, then the input and output connection relations will be such that R-phase is connected to U-phase and V-phase, and T-phase is connected to W-phase. Consequently, the matrix converter similarly turns on switches S_{ru}, S_{rv} and S_{tw}. As a result, R-phase is connected to U-phase and V-phase, and T-phase is connected to W-phase, and the operation of the matrix converter becomes same as that of the conventional PWM system.

Figure 7 shows waveforms of the matrix converter with the virtual indirect control method. The load is an induction motor. Unity power factor of the input is observed, and good sinusoidal waveforms were obtained for both the input and output currents.

Figure 8 shows the input power factor and total harmonic distortion (THD) of the input current versus load torque. The input power factor is more than 99 % at 50 % load torque or higher. THD of the input current is also less than 10 % at 50 % load torque or higher.

Figures 9 and 10 show waveforms of the acceleration-deceleration characteristic and impact load torque characteristic, respectively, in the case of using the vector control method for the induction motor control. The magnetizing current remains constant even when the torque current changes, and it can be verified that vector control achieves good results, similar to those of the conventional motor control. Moreover, during deceleration it can be seen that input current increases and power is regenerated.

4. Conclusion

New technology that enables the practical application of matrix converters has been introduced. Although not discussed in this paper, technical development is also underway to overcome the following basic limitations of the matrix converter.

(1) Since this is an AC-AC direct conversion method, the maximum voltage that can be output as a sinusoidal wave is limited to 0.866 times the input voltage.

(2) Since there is energy storage device, the matrix converter is susceptible to input voltage disturbances such as power failures.

Elevators and cranes, which require the regenerative operations, are suitable targets where the matrix converter is applied. Moreover, since the input current has low harmonic content, the matrix converter holds promise as a means to lessen current harmonics. Future application is also expected to fields that use PWM rectifiers and inverters, such as in a flywheel energy storage system. The RB-IGBT is expected to achieve even higher breakdown voltages and larger current capacity in the future, similar to that of the conventional IGBT. Along with these trends, the range of applications of the matrix converter is also expected to expand, and we intend to do our best to provide solutions.

References

(1) Takei, M. et al. The Reverse Blocking IGBT for Matrix Converter with Ultra-Thin Wafer Technology. Proceedings of the 15th International Symposium on Power Semiconductor Devices & ICs (ISPSD). 2003, p.156-159.

(2) Roy, M. et al. The MBS (MOS Bidirectional Switch), a new MOS switch with reverse blocking voltage. EPE99-Lausanne. 1999.

(3) Oyama, J. et al. New Control Strategy for Matrix Converter. Proceeding of Power Electronics Society Conference. 1989, p.360-367.

Global Network

AMERICA

● **FUJI ELECTRIC CORP. OF AMERICA**
USA
Tel : +1-201-712-0555 Fax : +1-201-368-8258

◆ **U.S. FUJI ELECTRIC INC.**
USA
Tel : +1-732-560-9410 Fax : +1-732-457-0042

◆ **FUJI HI-TECH, INC.**
USA
Tel : +1-510-651-0811 Fax : +1-510-651-9070

● **FUJI SEMICONDUCTOR, INC.**
USA
Tel : +1-972-733-1700 Fax : +1-972-381-9991

● **GE FUJI DRIVES USA, INC.**
USA
Tel : +1-540-387-5925 Fax : +1-540-387-8580

● **GE FUJI DRIVES AMERICA S.A, de C.V.**
MEXICO
Tel : +52-81-8-154-7000 Fax : +52-81-8-154-7007

EU

■ **FUJI ELECTRIC HOLDINGS CO., LTD.**
Erlangen Representative Office
F.R. GERMANY
Tel : +49-9131-729613 Fax : +49-9131-28831

● **FUJI ELECTRIC GmbH**
F.R. GERMANY
Tel : +49-69-6690290 Fax : +49-69-6661020

◆ **FUJI ELECTRIC (SCOTLAND) LTD.**
U.K.
Tel : +44-1355-234111 Fax : +44-1355-238810

◆ **FUJI ELECTRIC FRANCE S.A.**
FRANCE
Tel : +33-4-73-98-26-98 Fax : +33-4-73-98-26-99

ASIA

East Asia

■ **FUJI ELECTRIC HOLDINGS CO., LTD.**
China Representative Office (Shanghai)
THE PEOPLE'S REPUBLIC OF CHINA
Tel : +86-21-6471-0897 Fax : +86-21-6471-4903

■ **FUJI ELECTRIC HOLDINGS CO., LTD.**
China Representative Office (Beijing)
THE PEOPLE'S REPUBLIC OF CHINA
Tel : +86-10-6505-1263 Fax : +86-10-6505-1851

● **FUJI ELECTRIC (SHANGHAI) CO., LTD.**
THE PEOPLE'S REPUBLIC OF CHINA
Tel : +86-21-6466-2810 Fax : +86-21-6473-3292

◆ **FUJI ELECTRIC (CHANGSHU) CO., LTD.**
THE PEOPLE'S REPUBLIC OF CHINA
Tel : +86-512-5284-5629 Fax : +86-512-5284-5640

◆ **FUJI GE DRIVES (WUXI) CO., LTD.**
THE PEOPLE'S REPUBLIC OF CHINA
Tel : +86-510-528-1932 Fax : +86-510-528-2052

◆ **FUJI ELECTRIC DALIAN CO., LTD.**
THE PEOPLE'S REPUBLIC OF CHINA
Tel : +86-411-762-2000 Fax : +86-411-762-2030

◆ **SHANGHAI FUJI ELECTRIC SWITCHGEAR CO., LTD.**
THE PEOPLE'S REPUBLIC OF CHINA
Tel : +86-21-5718-5740 Fax : +86-21-5718-1448

◆ **SHANGHAI FUJI ELECTRIC TRANSFORMER CO., LTD.**
THE PEOPLE'S REPUBLIC OF CHINA
Tel : +86-21-5718-5747 Fax : +86-21-5718-5745

◆ **SHANGHAI GENERAL FUJI REFRIGERATION EQUIPMENT CO., LTD.**
THE PEOPLE'S REPUBLIC OF CHINA
Tel : +86-21-6921-1088 Fax : +86-21-6921-1066

◆ **HANGZHOU FUJI REFRIGERATING MACHINE CO., LTD.**
THE PEOPLE'S REPUBLIC OF CHINA
Tel : +86-571-8821-1661 Fax : +86-571-8821-0550

◆ **FUJI ELECTRIC (SHENZHEN) CO., LTD.**
THE PEOPLE'S REPUBLIC OF CHINA
Tel : +86-755-2737-4536 Fax : +86-755-2737-4535

◆ **HONG KONG FUJIDENKI CO., LTD.**
HONG KONG
Tel : +852-2664-8699 Fax : +852-2664-8040

● **FUJI ELECTRIC (ASIA) CO., LTD.**
HONG KONG
Tel : +852-2313-7900 Fax : +852-2312-0566

■ **FUJI ELECTRIC SYSTEMS CO., LTD.**
Taipei Representative Office
TAIWAN
Tel : +886-2-2561-1256 Fax : +886-2-2561-0528

● **FUJI ELECTRIC TAIWAN CO., LTD.**
TAIWAN
Tel : +886-2-2515-1850 Fax : +886-2-2515-1860

● **FUJI/GE TAIWAN CO., LTD.**
TAIWAN
Tel : +886-2-2556-0716 Fax : +886-2-2556-0717

◆ **ATAI FUJI ELECTRIC CO., LTD.**
TAIWAN
Tel : +886-3-321-3030 Fax : +886-3-321-7890

● **FUJI ELECTRIC KOREA CO., LTD.**
KOREA
Tel : +82-2-780-5011 Fax : +82-2-783-1707

Southeast Asia

■ **FUJI ELECTRIC SYSTEMS CO., LTD.**
Bangkok Representative Office
THAILAND
Tel : +66-2-308-2240, 2241 Fax : +66-2-308-2242

■ **FUJI ELECTRIC SYSTEMS CO., LTD.**
Jakarta Representative Office
INDONESIA
Tel : +62-21-572-4281 Fax : +62-21-572-4283

◆ **FUJI ELECTRIC (MALAYSIA) SDN. BHD.**
MALAYSIA
Tel : +60-4-403-1111 Fax : +60-4-403-1496

◆ **FUJI ELECTRIC PHILIPPINES, INC.**
PHILIPPINES
Tel : +63-2-844-6183 Fax : +63-2-844-6196

● **FUJI ELECTRIC SINGAPORE PRIVATE LTD.**
SINGAPORE
Tel : +65-6535-8998 Fax : +65-6532-6866

◆ **FUJI/GE PRIVATE LTD.**
SINGAPORE
Tel : +65-6533-0010 Fax : +65-6533-0021

e-Front runners

Printed on recycled paper